CRUISE REPORT

POSEIDON Eurofleet+

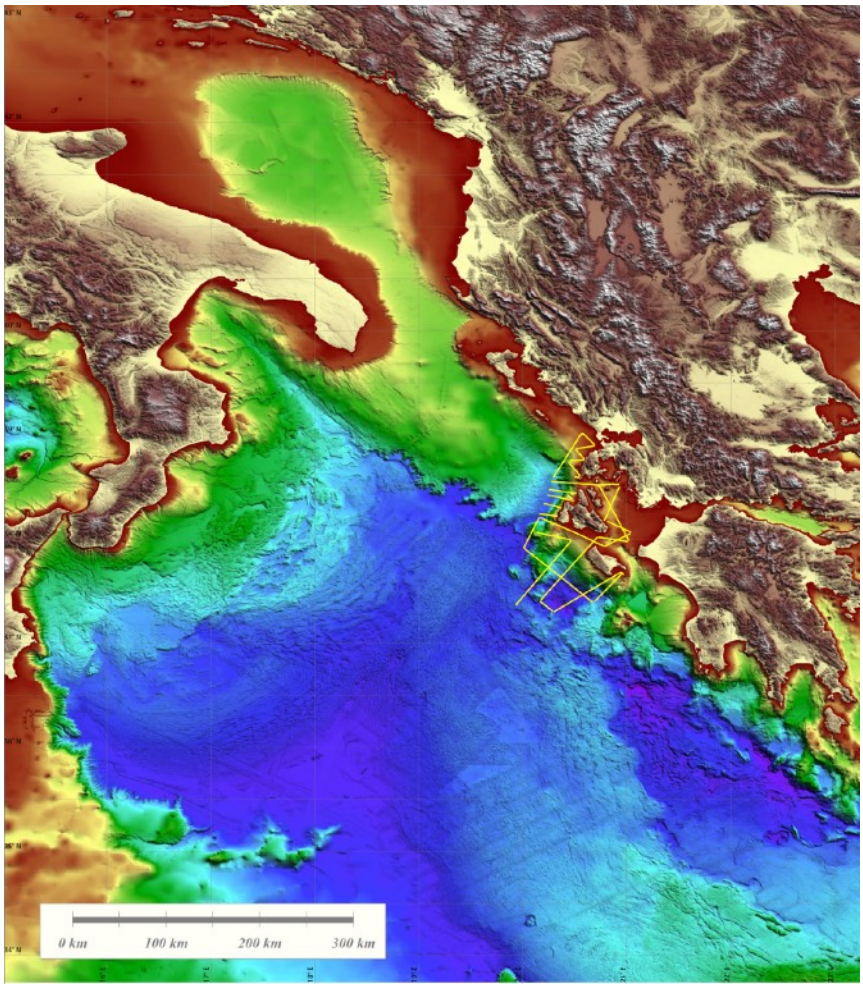

R/V Laura Bassi 10 – 22 June 2023

Chief Scientists:

C.R. Ranero - P. Nomikou - F. Loreto

Barcelona CSI Center for Subsurface Imaging

CSIC Consejo Superior de Investigaciones Científicas

Institut de Ciències del Mar

ICREA

Laboratory of Physical Geography

Hellenic Republic National and Kapodistrian University of Athens Est. 1837

CNR ISMAR Istituto di Scienze Marine

INTRODUCTION

The POSEIDON cruise comprised the acquisition of marine geophysical as a collaborative effort of Spanish, Italian and Greek scientist under the umbrella of the Eurofleet+ program onboard Italian Research Vessel Laura Bassi.

POSEIDON aims at studying arguably one of the most complex and comparatively little evaluated regions with demonstrated high seismic hazard in the Mediterranean: The western Peloponnese & Ionian Islands tectonic domain. Here, a complex fault system occurs across an area with a dramatic change in deformation rates, purportedly near the end of the Hellenic subduction zone. The fault system produces numerous large earthquakes, mostly offshore, recorded in the onshore Greek seismological network during the last decades. However, some events are poorly known, like the Cephalonia 1953 Mw~6.8 event, possibly the most destructive earthquake in recent Greek history. The 1953 event caused the collapse of 85% of all buildings on the Island of Cephalonia, ~1000 deaths, and ~145k homeless, and initiated a long-term population migration affecting the local economy, that has only recently started to heal. The earthquake was recorded in few stations causing that even today it has a poorly located epicenter, let alone the hypocenter depth.

Even today, the causative fault is unknown, which is aggravated because the tectonic map of the region remains poorly defined. Here, the location, dimension and kinematics of the main fault structures is only sketchy, let alone their deep structure. A thrust-fault focal mechanism E-SE of Cephalonia is proposed to have caused the 1953 event with a hypocenter depth between <50 km to <20 km, depending on the analysis. However, geological studies onshore in the islands propose that active shallow (<~5 km) thrusting ruptured by the 1953 event.

Limited high resolution bathymetry available to date across much of the region indicates complex fault structure and kinematics. An upper-crust fault system may have developed above a mega-thrust fault of the Hellenic subduction zone. However, the definition of the mega-thrust fault is poor and has been inferred to dip NE at ~25-40 km depth under the islands. Nonetheless, a plate boundary fault has not being clearly imaged or mapped and its geometry and relation to the seismicity is largely speculative. Thus, the transition from the upper-crust seismogenic zone to the mega-thrust is not understood.

The POSEIDON research region has developed above the edge of the subducting slab, which is bounded to the NW by a tear. So that we have the opportunity to study the early stages of a Subduction-Transform Edge Propagator (STEP) fault system. POSEIDON aims are threefold and will A) Answer major open issues regarding faulting and natural hazards in the region, B) Address fundamental questions of earthquake phenomena, and C) Expand understanding in basic research related to subduction systems and STEP evolution.

1. PARTICIPANTS

1.1. Chief-scientists

César R. Ranero - Consejo Superior de Investigaciones Científicas (CSIC) Institut de Ciències del Mar (ICM) Passeig Marítim de la Barceloneta, 37-49, 08003 Barcelona (Spain)
Phone: +34 93 230 96 23 /+34 93 230 95 00
E-mail: cranero@icm.csic.es

Filomena Loreto - CNR Bologna (Italy)

Paraskevi Nomikou - National & Kapodistrian University of Athens Department of Geology & Geoenvironment Division of Geography & Climatology Laboratory of Physical Geography, Panepistimiopolis, Zographou 157 84 Athens, (Greece)
Phone: +30 210 7274865
E-mail: evinom@geol.uoa.gr

1.2. Science party

César Ranero	Marine Geophysicist ICREA-CSIC Barcelona	Chief scientist
Filomena Loreto	Marine Geologist CNR Bologna	Co-chief scientist
Paraskevi Nomikou	Marine Geologist Uni. Athens	Co-chief scientist
Irene Merino	Marine Geophysicist ICM-CSIC Barcelona	Seismic Processing
Danai Lampridou	Marine Hydrographer Uni. Athens	Multibeam echo sounder
Elisavet Nikoli	Marine Hydrographer Uni. Athens	Multibeam echo sounder

Valentina Ferrante	Marine Geologist CNR Bologna	Parametric echo sounder
Serafim Poulos	Marine Geologist Univ. Athens	Sediment coring
Giota Giogli	Marine Biologist GeoMar, Greece	Marine Mammal Observer

1.3. Technical team CSIC (Spain)

Ramon Ametller	UTM-CSIC	Compressor
Mario Sánchez	UTM-CSIC	Compressor

1.4. Technical team OGS Trieste (Spain)

Roberto Romeo	OGS	Party chief
Lorenzo Facchin	OGS	Seismic acquisition
Paolo Visnovic	OGS	Seismic acquisition
Alessandro Bubi	OGS	Seismic acquisition
Fabrizio Zgur	OGS	Seismic acquisition
Andrea Cova	OGS	Seismic acquisition
Michela Dal Cin	OGS	Topas Acquisition
Daniela Accettella	OGS	Multibeam bathymetry
Marco Santulin	OGS	Multibeam bathymetry
Matilde Ferrante	OGS	Multibeam bathymetry

1.5. Participating institutions of Scientific Crew

ICM-CSIC Institute of Marine Sciences CSIC Centre Mediterrani d'Investigacions Marines i Ambientals Passeig Marítim de la Barceloneta, 37-49 08003 Barcelona | Spain	
ICREA Catalan Institution for Research and Advanced Studies Passeig Lluís Companys 23 08010 Barcelona, Spain	
CNR *Bologna* *Via Piero Gobetti, 101, 40129 Bologna BO, Italy*	
University of Athens Zographou 157 84 Athens, (Greece)	
Geo-Mar *Greece and UK*	

2. SCIENTIFIC RATIONALE

2.1. Current state of scientific knowledge

Research of earthquake-related phenomena remains a priority in Earth Sciences. The largest earthquakes occur at subduction zones during rupture of plate-boundary faults between under-thrusting and overriding plates. Earthquakes occur there more often than anywhere else, causing intense deformation and the biggest tsunamis, and therefore the highest economic losses and casualties. Our knowledge of the processes that govern earthquake seismogenesis has been periodically synthesized during the past ~40 years into different conceptual models to provide a basic framework for testing and advance in the understanding of the earthquake phenomena.

A basic concept is that opposed lithospheric plates are mechanically (partially) locked in a portion of the fault that forms the contact. This locked segment is the so-called *seismogenic zone,* which controls the region where elastic energy gradually accumulates, and their spatial dimensions influences the greatest-possible magnitude for earthquakes (e.g. Wang et al., 2012; Herrendörfer et al., 2015). Updip and downdip of the *seismogenic zone* the plates are inferred to slip by slow slip phenomena, in ways recognised during the last decade (Lay et al., 2012).

To our disconcert, most fundamental forecasts put forward by those hypotheses have been falsified by the unexpected characteristics of several great earthquakes during the last ~15 years. Early concepts proposed that the greatest earthquakes should occur in fast-converging subduction zones with thick trench-sediment packages, which when subducted should smooth the mega-thrust fault structure and facilitate propagation of rupture. This hypothesis was partially disproven during the 2004 Aceh-Andaman Mw9.3 event, occurring along a segment of the obliquely (slowly) converging Sumatra subduction zone (Lay et al., 2005). More recently, the 2011 Tohoku-Oki Mw9.0 event ruptured along a plate boundary with a thin veneer of subducted sediment, indicating that a laterally homogeneous mega-thrust fault is not required for the generation of great earthquakes (Fujiwara et al., 2011).

The modern and abundant high-quality seismological data has also been used to show that a number of other frequently (and freely) utilized concepts are primarily incorrect. For instance, the 2011 Tohoku-Oki M_w9.0 event re-ruptured a region also partially ruptured few years before by preceding M_w8.0-8.5 events. Such M_w8.0-8.5 earthquakes were previously frequently inferred as “large enough” to release most of the stress. The Tohoku-Oki M_w9.0 event - and paleoseismic data - support that, at least in some regions, the release of elastic energy may follow a cycle that is more complex that previously assumed. In Japan Trench, and possibly other regions like Cascadia, a decadal-centennial cycle of ~M_w8.0-8.5 great earthquakes may be “superimposed” to a longer-time scale cycle (perhaps millennia) of >M_w9.0 giant earthquakes.

A last failed hypothesis worth mentioning of this ongoing paradigm shift is the very concept of the seismogenic zone: mounting evidence supports that it has been too simplistically applied to the complex fault behavior occurring during earthquake nucleation, rupture and propagation. High-quality records inverted to map fault rupture of recent great earthquakes including Aceh-Andaman, Tohoku-Oki, and Maule (Chile) strongly indicate that rupture extended along the shallow portion of the faults to reach close to the deformation front (Fujiwara et al., 2011, Maksymowicz, et al. 2017), where conceptual models infer that

deformation normally occurs a-seismically. The shallow slip for all those earthquakes caused deformation that produced unexpectedly-large tsunamis of dimensions that require that the amount of slip peaked at the shallow region, near the trench axis (Sun et al., 2017).

The above brief background points to a growing body of evidence showing our insufficient understanding of fault mechanics and deformation at the scale of plate-boundary faults, which has led to long-standing, oversimplified conceptual models.

Plate-boundary faults capable of generating great earthquakes are also formed by strike-slip thousands-of-km-long fault systems in continental settings, like the well-developed San Andreas fault, Queen Charlotte fault, Sumatra fault. However, there are regions where more complex sets of faults forms the plate boundary: The fault system along much of the contact between African and European plates is relatively well known when occurs onshore, but poorly known in many submarine areas, lacking basic information such as major fault structure, fault slip rates, and often lacking the information on the elastic structure of the crust.

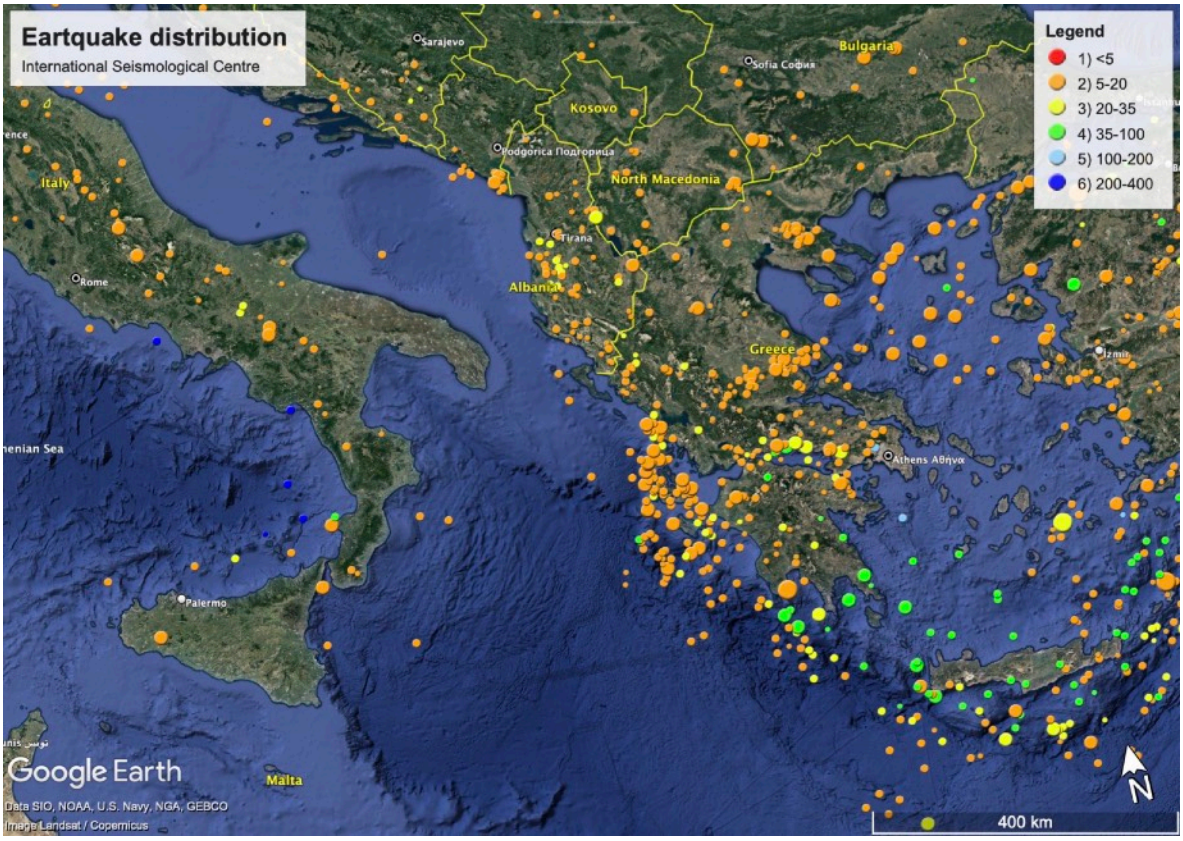

Fig 1, *Recent seismicity from the International Seismological Centre. The POSEIDON study region of the Ionian Greek islands displays the highest earthquake density of the Mediterranean realm.*

Our group and collaborators have used multi-scale methodological approaches, combining different resolutions, to show how recent large earthquakes are associated to complex submarine fault systems in the western Mediterranean, revealing under-evaluated hazards (e.g. Gràcia et al., 2019, Gomez de la Peña et al., 2022). Offshore mapping, and recently monitoring, of the North Anatolian Fault evaluate its impending hazard (e.g. Lange et al,

2019), but no other offshore Mediterranean plate boundaries have attracted similar dedicated international research.

POSEIDON aims at studying arguably one of the most complex and comparatively little evaluated regions with demonstrated seismic hazard, which extends across the western Peloponnese and Ionian Islands tectonic domain (Figure 1).

A complex fault system has developed (Fig 2a) in a region with a dramatic change in deformation rates (Fig 1b). This system has produced numerous large earthquakes, mostly offshore, recorded in the onshore Greek national seismological network (Fig 2a) (Hadad et al., 2020). However, the Cephalonia 1953 M_w~6.8 event (Stiros et al., 1994) occurred when Greece was coming out of a civil and was recorded in comparatively few stations only. This earthquake is possibly the most destructive seismic event in recent Greek history, causing the collapse of 85% of all buildings on Cephalonia, ~1000 deaths, and ~145k people homeless, and initiated a long-term migration of the population, with effects in the local economy that only recently started to heal (Saranga, 2017; Hore, 2019). The limited data on the 1953 earthquake has made it comparatively poorly understood: the epicenter is poorly located and the causative fault is disputable. Likewise, the thrust fault focal mechanism, located E or SE of Cephalonia, has a hypocenter depth poorly defined from <50 km to <20 km, depending on the analysis. In contrast, surface geology studies of the islands (Underhill, 1989) interpreted active shallow thrusting, and it has been proposed that the 1953 event ruptured several of those faults (Fig 2c). To determine region fault system structure and kinematics, requires further work.

The available modern bathymetric mapping supports that in region from the Ionian Islands to the Peloponnese Peninsula there is active deformation on structures trending NW-SE, trending similar to the basin and ranges and linear coastlines of the islands (Figure 1a). Unfortunately, little available seismic data imaging those structures. A fold and thrust belt is recognized onshore (Underhill, 1989), and it has been imaged offshore in a bay SW of Cephalonia Island, where folds appear inactive structures, eroded and covered by Quaternary-to-recent unfolded sediment (Underhill, 2009). However, the elongated shallow troughs offshore that laterally project into the morphological trends of the islands, do not support widespread thrust faulting, as proposed for the 1953 dramatic event. The seafloor relief could potentially represent structures with a strike-slip to oblique component that kinematically link onshore and offshore structures, with changes from transtension to oblique thrust component along strike, but this is not reflected in the published mechanisms.

An additional complexity to POSEIDON research area is that the upper-crust fault system discussed above, might be located above the mega-thrust fault of the Hellenic subduction zone, inferred to dip NE at ~25-40 km depth under the surface (Hansen et al., 2019, Haddad et al., 2020). The transition from the upper-crust seismogenic zone to the mega-thrust seismogenic zone is not understood (Karastathis et al, 2015; Chousianitis & Konca 2019; Cirella et al, 2020). Thus, we may speculate that the devastating 1953 thrust earthquake may have ruptured a major splay fault, i.e. relatively steep, with surface expression, but rooting at the mega-thrust. But there are not seismic images to test it.

The area of the POSEIDON study has developed above the edge of the Ionian subducting slab, which is bounded to the NW by a tear (Hansen et al., 2019). So that in POSEIDON we have the opportunity to study the (early) stages of a Subduction-Transform Edge Propagator (STEP) fault system (Govers & Wortel, 2005). This scenario is supported by imaging of the

slab structure (Hansen et al., 2019), and agrees with the abrupt lateral change in the overriding plate deformation (Fig. 1b). Understanding the large-scale structure will be key to evaluate fault kinematics interpretation and model deformation numerically.

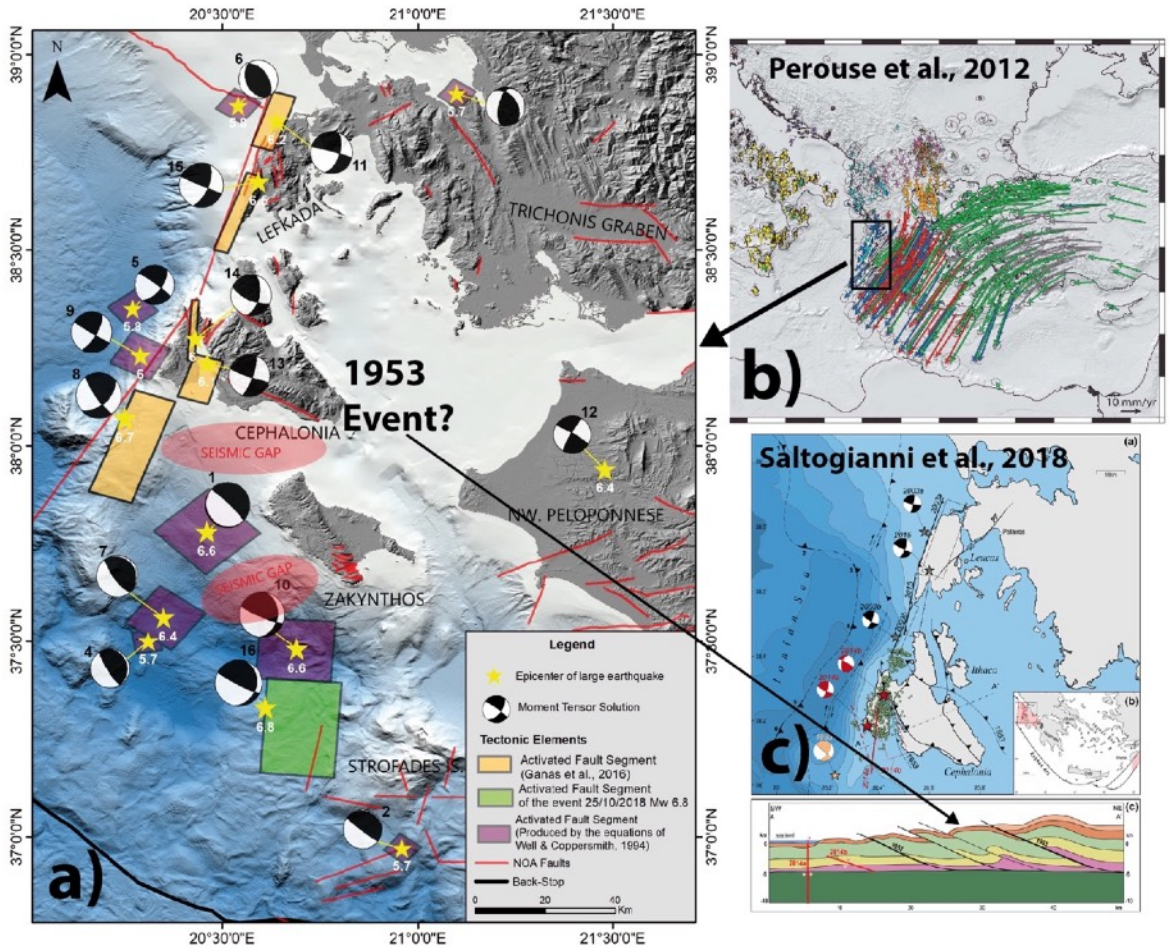

Fig 2, a) *Recent earthquakes (Ganas et al. 2021),* ***b)*** *GPS velocities in Eurasia fixed reference frame with their respective 95% confidence ellipse,* ***c)*** *Cross section Interpretation of shallow structure.*

2.2. Specific aims of the POSEIDON research project

POSEIDON aims at answering major open issues regarding *active faulting*, to provide a database to improve the *assessment of natural hazards* in the region, and to expand understanding in basic research related to subduction systems and *STEP evolution*. Each of these three aims contain several specific goals:

Active Faulting: POSEIDON aims at, for the first time, map the offshore fault geometry and kinematics using multi-beam bathymetry, seismic imaging. Carefully located sediment cores will help to determine the geochemical tracers of potential re-sedimented layers related to the main regional earthquakes. High resolution swath mapping, combined with sub-bottom profiles will allow to produce a detailed morpho-structural map of the main NE-trending Cephalonia fault system, that on its northern part is still unknown. A middle resolution seismic grid will provide the first detailed map of the major offshore faults distribution, segment dimensions and their linkage to onshore structures of the Peloponnese.

Assesment of natural hazards: The kinematics of faults will be integrated using characteristic geological markers in seismic and GPS information (Fig. 1b). The seismo-tectonic map will integrate tectonics with seismicity to evaluate hazard of major faults. Of particular interest is to understand the relationship of the 1953 event and upper crust faulting. The mapping of the dimensions of the major faults will be of great interest to evaluate and improve the assessment of earthquake-related natural hazards in the region.

STEP evolution: The anticipated major improvement in our understanding of the fault structure and kinematics and crustal elastic properties will be the basis for a new mechanical (4D) model, with which we aim to identify how slip deficit partitions on splay faults and the subduction megathrust. Tectonically, the source area of the regional earthquakes and tsunamis is complex as it includes the active Kefalonia STEP fault and the associated complexity in slab structure (Govers and Wortel, 2005; Özbakır, 2019). The regional model will be used to assimilate observations of active kinematics (i.e. focal mechanisms, geodetic velocity) of the current interseismic period, to then extend over multiple earthquake cycles to assimilate data (e.g., terrace uplift and permanent deformation of the overriding plate) over the longer term geological history, covering multiple earthquake cycles.

3. INSTRUMENTATION

In this section are described the characteristics of the equipment used for seismic acquisition during the POSEIDON cruise.

3.1 Instrumentation for seismic data acquisition

3.1.1 Streamer

The Multichannel streamer SENTINEL from Sercel contains the hydrophone sensors used to receive the acoustic signal from the guns. Each seismic channel corresponds to a group of hydrophones, that are associated with electronic devices responsible for adequately manage the acquired signal or data. The streamer has a 59.5 mm diameter and 150m-length active sections with 12 channels (each 12.5 m length) that receive the information of 8 hydrophones. These active sections also contain of passive segments with acquisition and control modules. The streamer on Laura Bassi is 1500 metres long and was deployed at 7 m depth.

Figure 3: Multichannel streamer SENTINEL Sercel (yellow hose) on the lower deck of R/V Laura Bassi.

3.1.2 Seismic source

MCS acquisition during the POSEIDON cruise used as seismic source composed of an airgun array with 1000 c. i. total volume (Table 1), deployed at a depth of 5 m, in *Figure YY*.

The compressor adequate for the cruise was not available ion the R/V Laura Bassi. We installed an LMF compressor from Spanish CSIC with 2 technicians for maintenance for the source. The compressor provided air for shooting every 37.5 m.

Table 1: Airgun array characteristics.	
Number of airguns	4
Strings	1
Used volumes	250+250+250+250
Pressure	2000 psi
TOTAL volume	1000 c.i.

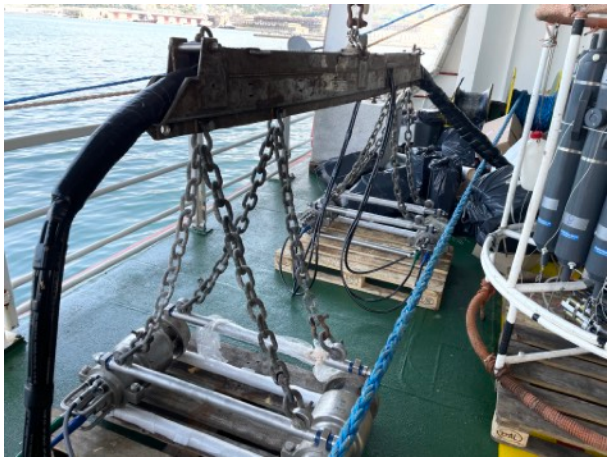

Figure 4a: Airgun array with 4 guns onboard R/V Laura Bassi,

Figure 4b: LMF compressor from Spanish CSIC installed on R/V Laura Bassi.

4. SEISMIC REFLECTION DATA: Onboard Processing

During the POSEIDON cruise we acquired 26 seismic lines designed to map the main tectonic features that were interpreted from the distribution of morphological features interpreted from the available bathymetry and the integration of bathymetry collected during the cruise (Figure 5).

The 26 seismic lines were processed onboard in parallel with the acquisition with a basic sequence (Table 2) to determine their quality and the penetration of the seismic signal and thus to consequently plan the acquisition across structures of interest.

Processing was aimed at obtaining a stack after careful velocity picking every 2.5 km and locally at shorter distance where the structure changes laterally rapidly. After velocity picking a Radon filter further attenuated the multiple. A hand-picked Vp model following the geology, using the smooth Vint version from the Vrms was used to FD post-stack migration of the images (Figures 6-XX).

The acquisition maps (Figure 5) shows that the lines were collected in the domains with different morphotectonic characteristics. One set of lines designed to map the Cephalonia fault structure along possibly all its length, located along the escarpments west of the Islands and that must extent into the continental platform. A second set of lines were collected between the Islands and the Peloponnese mainland to maps the tectonic features that are forming a series of elongated and narrow basins across the broad continental shelf. A third set of lines was collected south of Cephalonia and Zakynthos Islands to structure the transition from the shelf and Island topography to the deep water basin across a relatively narrow steep slope.

In this report we show a few examples. The seismic profiles show a rather complex and changing geology across the region (Figures 6-8). The acoustic source produced enough energy to be able to image along all sections the sedimentary cover and the top of a basement that may be formed by metamorphic, magmatic or perhaps mesozoic sediment in some areas. The seismic images display some deep reflection with the basement in some regions at ~4-7 seconds Two Way Travel Time (TWT) that might represent the Moho or deep intra-basement tectonic boundaries.

Table 2. Onboard Processing sequence
Read segD data
Insert regular marine geometry
Sorting to Common Mid Point (CMP) Gathers
Brute stack with Vp geologic model (produce CMP for Vp picking)
Picking semblance to determine Vp functions with preprocessed gathers
Spherical divergence correction
Radon Multiple Attenuation
Band pass Butterworth filter
Amplitude balance
Median Stack
Post stack FD migration (Vp geologic model)
Automatic Gain Control for display (2000 ms double median)

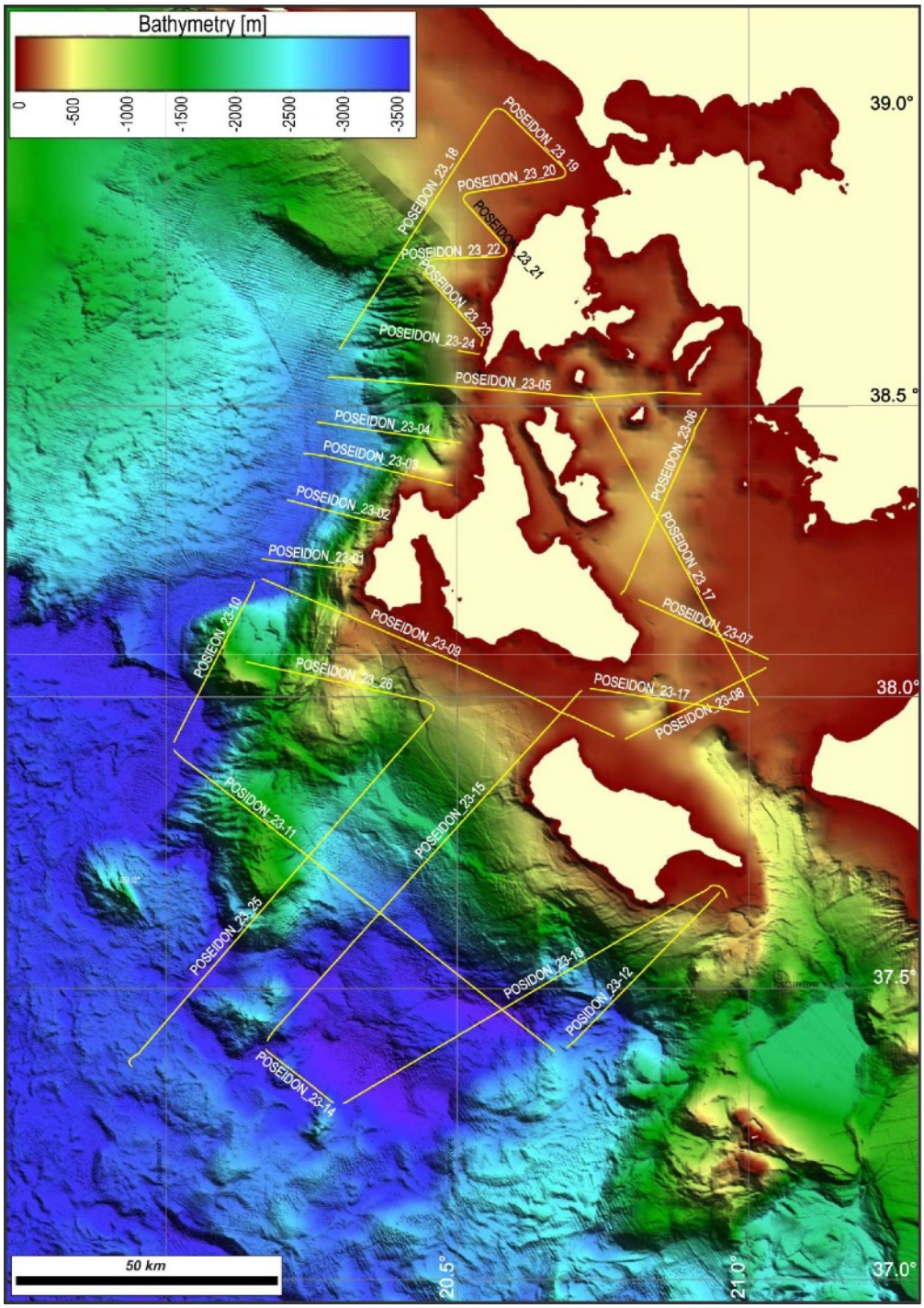

Figure 9. Bathymetric map of the study area with seismic profiles

Poseidon01-mig_vel1.hdf5

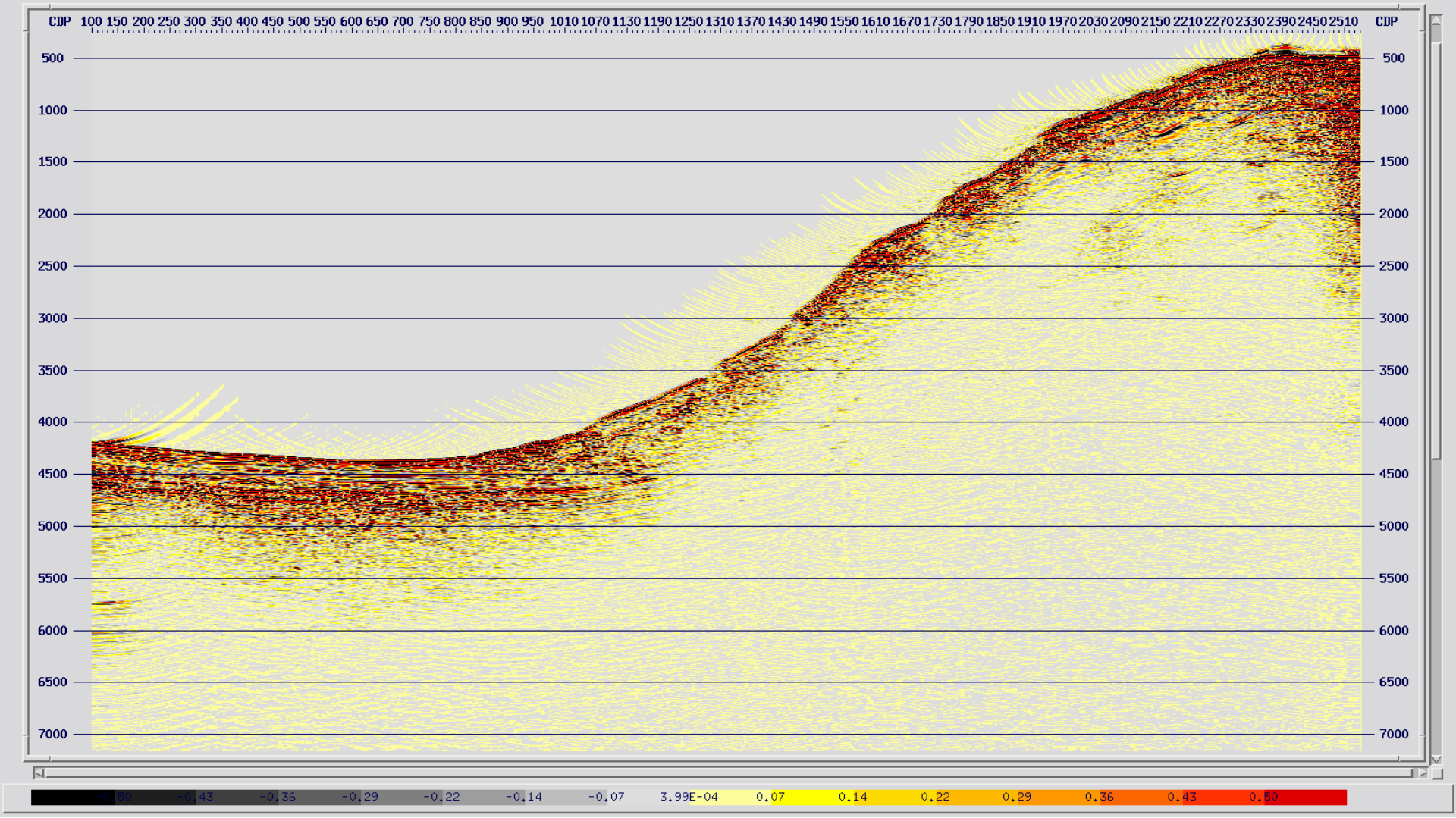

Figure 6

Close-up: Poseidon01-mig_vel1.hdf5

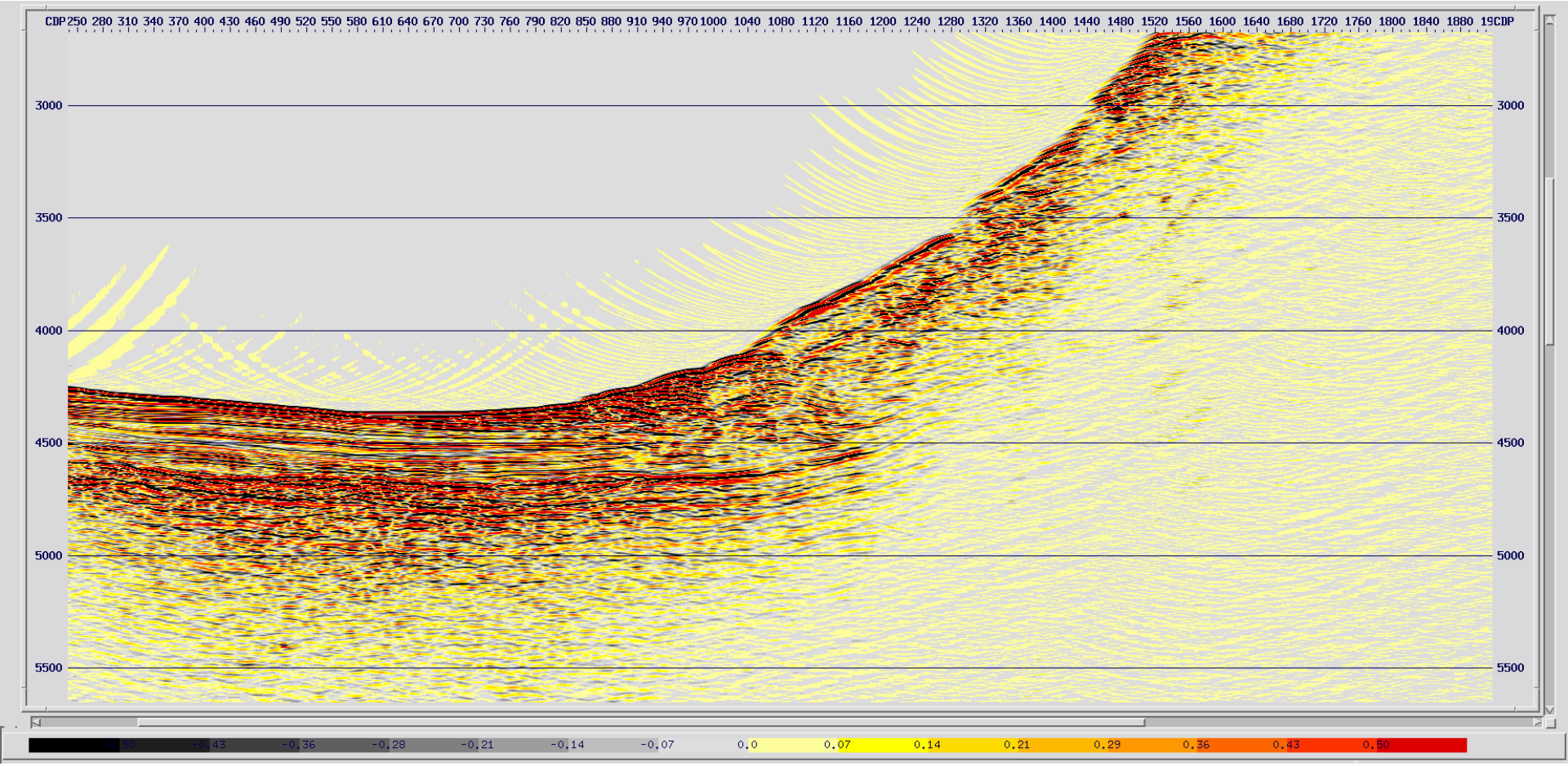

Figure 7

Poseidon02-mig_vel1.hdf5

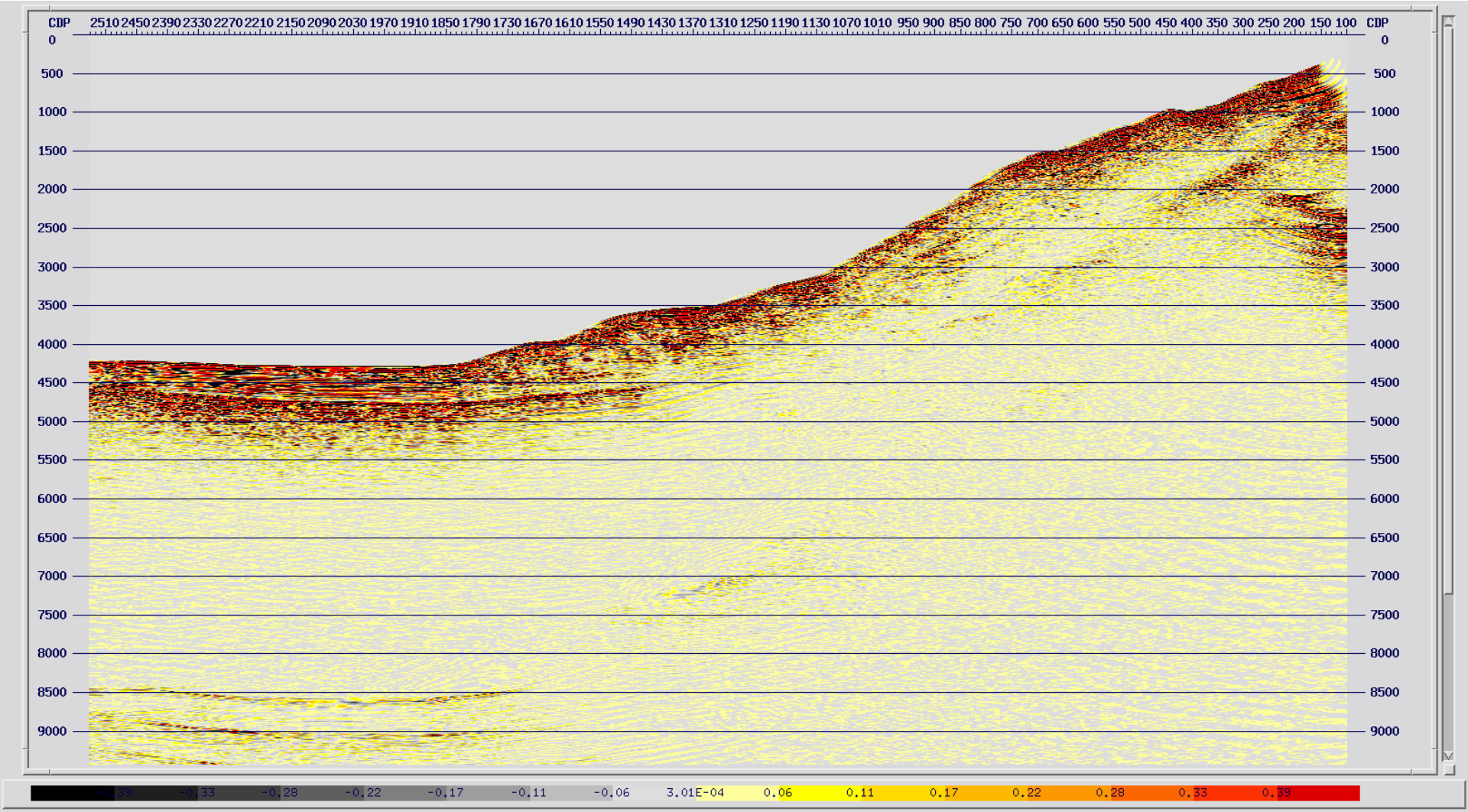

Figure 8

5. COMPLEMENTARY GEOPHYSICAL METHODS

During the POSEIDON survey, complementary acoustic data including multibeam bathymetry and parasound were acquired during seismic acquisition and a dedicated mutlibeam bathymetry survey to map the Cephalonia fault (Figures 40-43).

5.1 Bathymetry – Acquisition and Processing

During the POSEIDON 2023 cruise, swath data of approximately 1940 kilometers was collected around the Ionian Islands, including Zakynthos, Kefalonia, and Lefkada. The data was acquired using the hull-mounted multibeam Kongsberg EM304, operating at a nominal frequency of 30Khz. Throughout the acquisition process, adjustments were made to the gates and sector coverage to maximize the swath width while minimizing any inaccurate outer beams. To prevent interference, both the multibeam and TOPAS PS18 instruments were synchronized using K-sync.

A sound velocity profile was also obtained to reduce refraction errors. The data was acquired using two different software programs, namely SIS V5.9.3 and Quincy V9. Consequently, the data was saved in two distinct formats, *.kmall and *.db. In addition to bathymetry, snippets and water column data (>500m water depth) were recorded.

Qimera V2.5 was used for all multibeam data processing tasks, including sound speed corrections, line cleaning, and CUBE surface creation. The data was gridded at a resolution of 25 meters using the "deep configuration" CUBE settings. This specific configuration was chosen to enhance the likelihood of creating separate hypotheses for any erroneous beams encountered during the processing, thereby improving the accuracy and reliability of the final results.

5.2 Bathymetry – Preliminary results

The recently obtained high-resolution bathymetric data has provided insights into the intricate topography of the surveyed area. Specifically, the slope delineating Kefalonia Island is quite abrupt, with locally reaching slope values of approximately 30 degrees.

Moving towards the north, offshore Lefkada, the slope can be divided into two distinct branches:

a) A relatively flat region with its boundary at approximately 600 meters water depth. Within this area, a notable field of sediment waves is observed in the northern part.

b) Below the 600-meter water depth mark, the slope is significantly carved by canyons that trend in the NE-SW direction. The flanks of these canyons exhibit multiple coalescent and nested landslides.

To the southwest of Zakynthos, the area is also impacted by landslides. Additionally, two elongated basins are observed at water depths of 4230 and 4220 meters respectively.

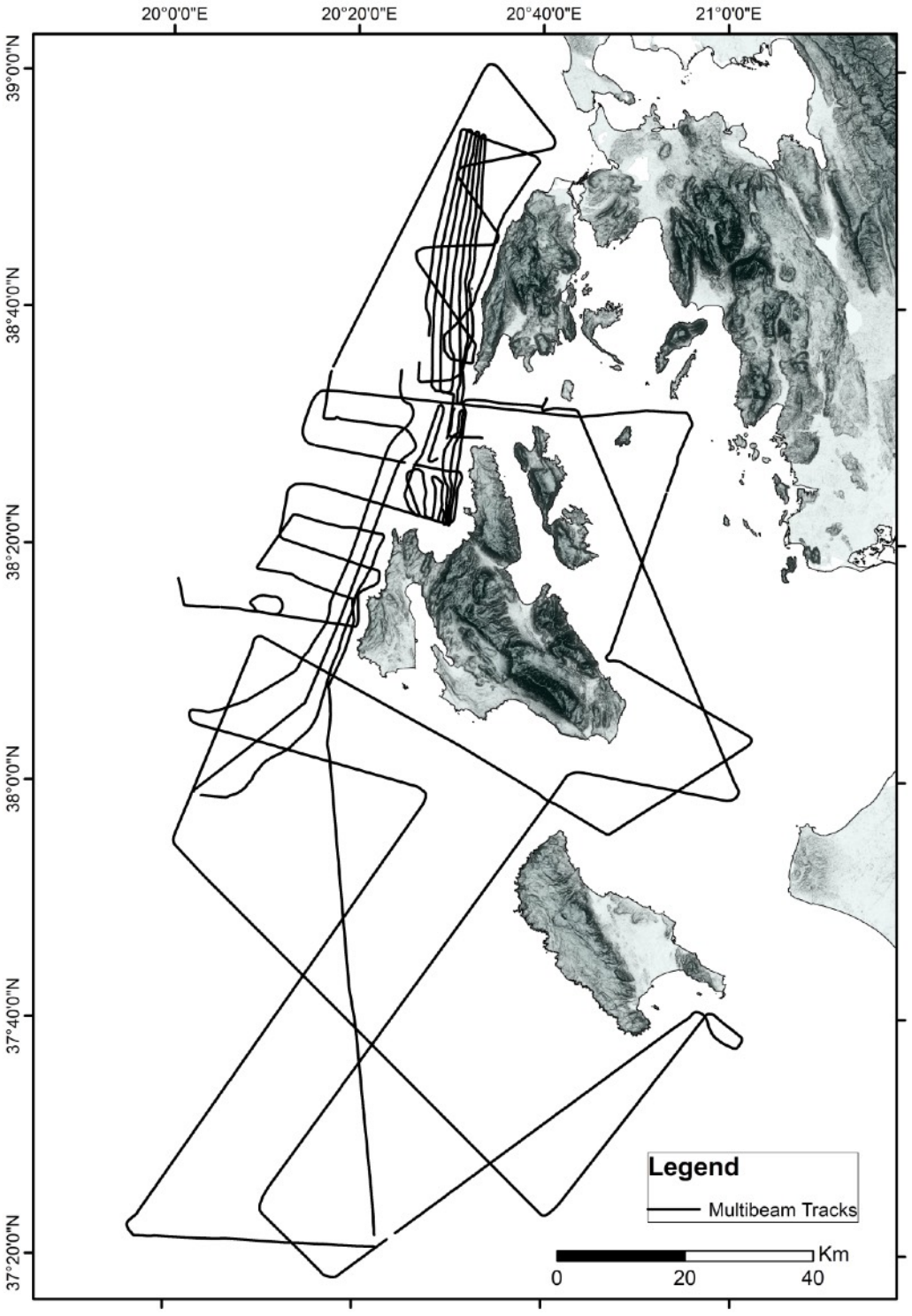

Figure 10: Tracks with multibeam bathymetry data acquired during the POSEIDON survey.

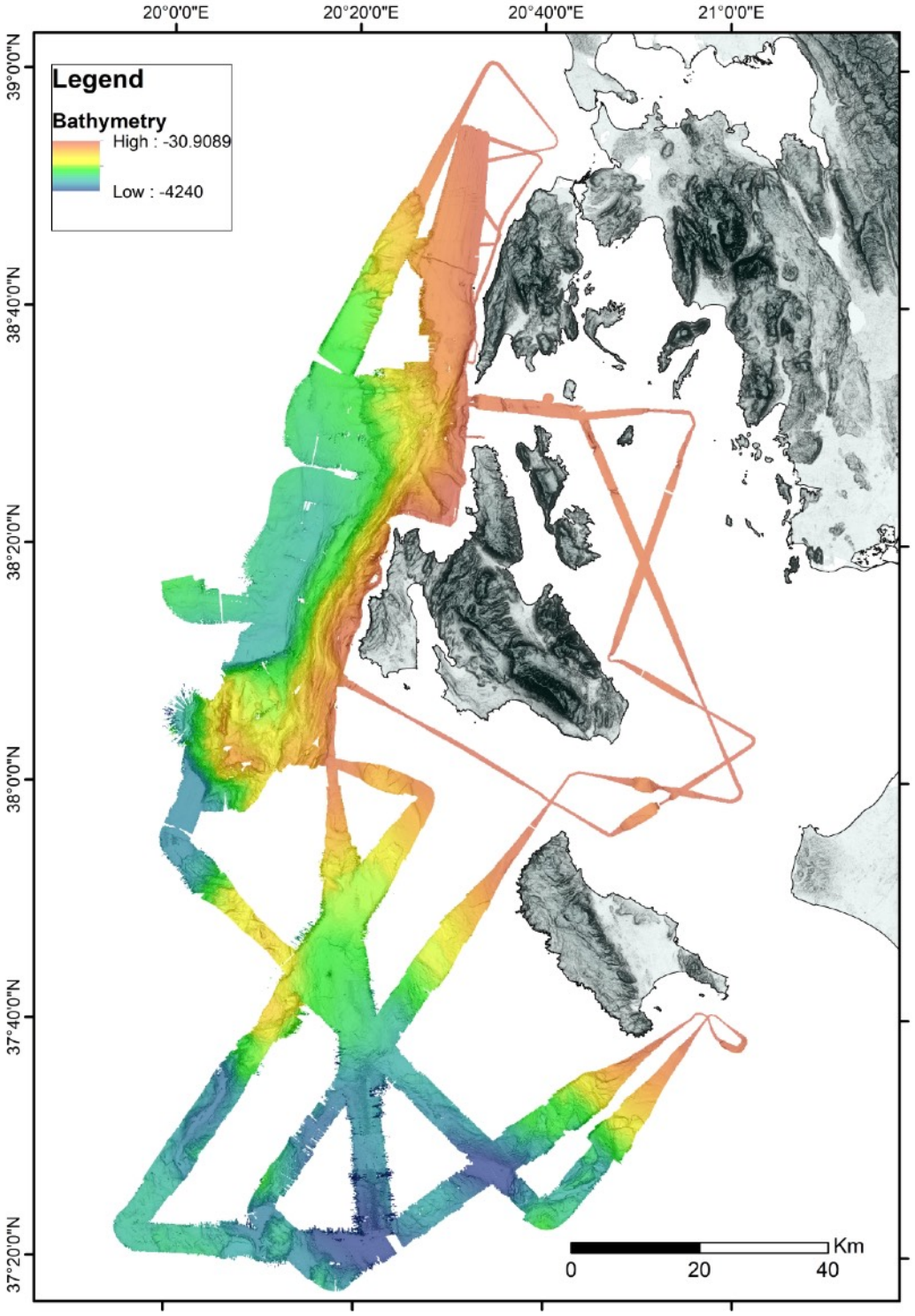

Figure 11: Multibeam bathymetry map with the data acquired during the POSEIDON survey.

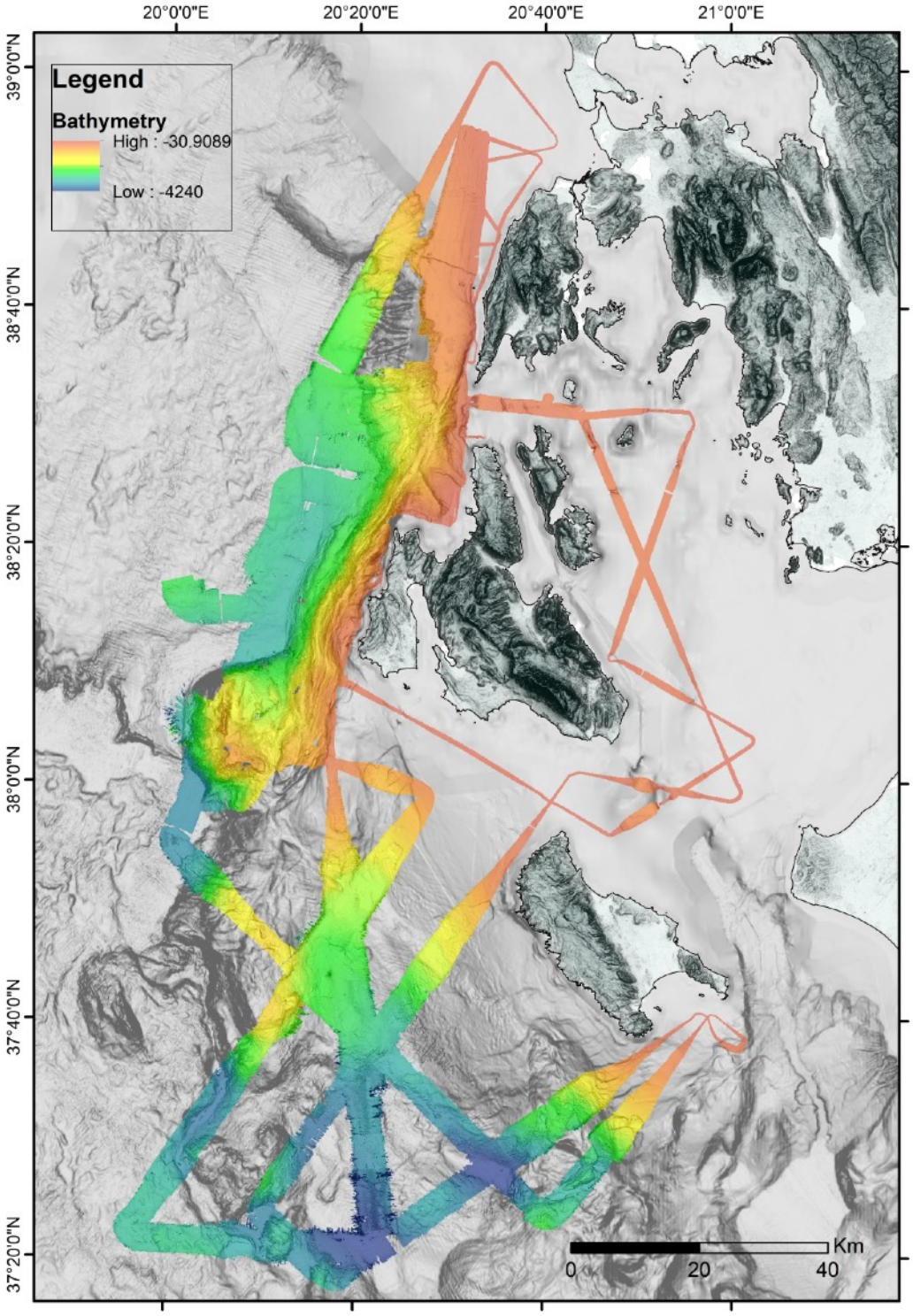

Figure 12: Multibeam bathymetry map with data acquired during the POSEIDON survey using an orange to blue color scale overlaid on grey shaded existing bathymetry.

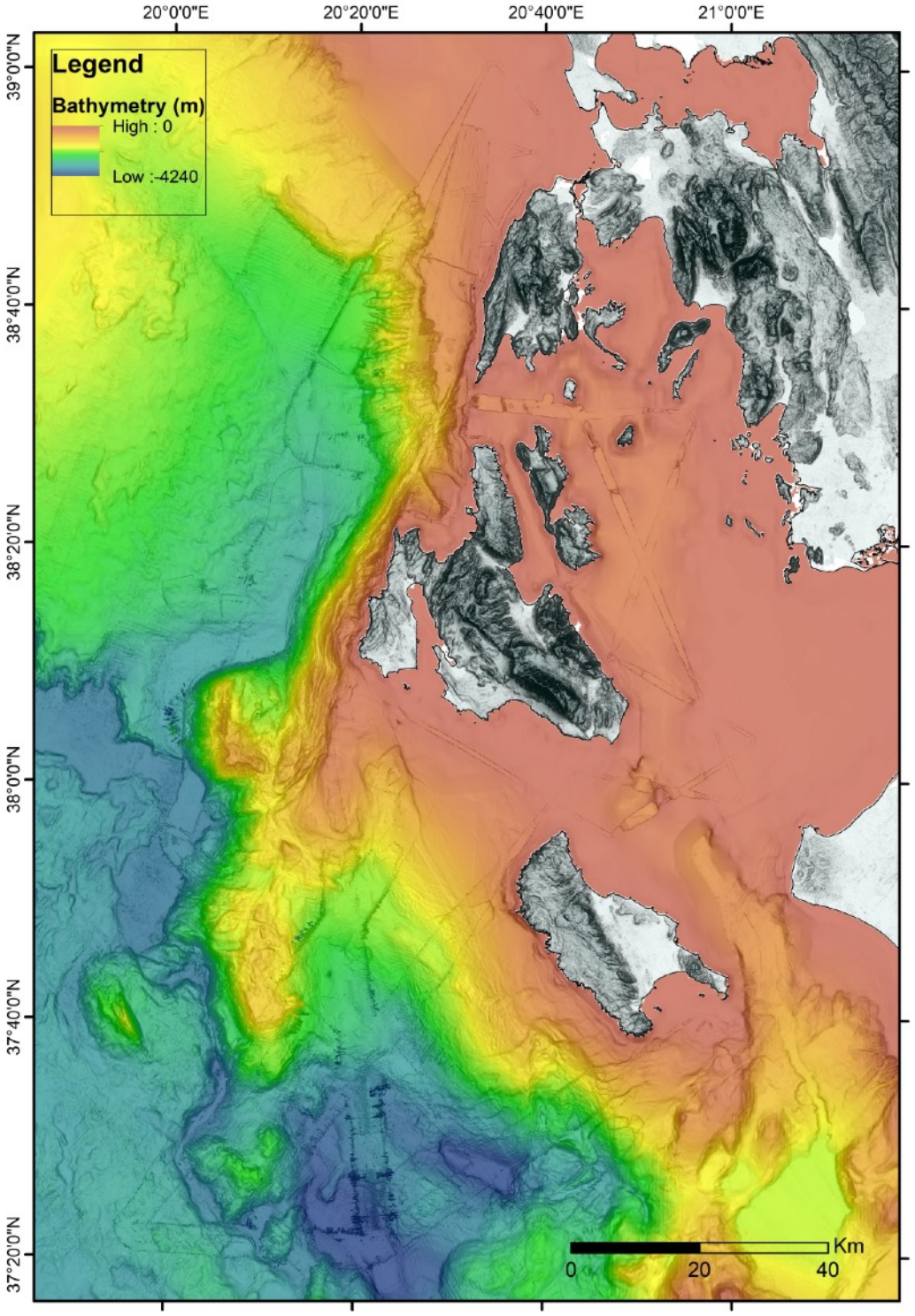

Figure 13: Multibeam bathymetry map integrating the data acquired during the POSEIDON survey with the available bathymetric data from previous cruises, all data with an orange to blue color scale, a topographic relief in grey shaded relief .

5.2 Parametric echo-sounder

Parametric echo sounder was collected along the entire cruise (Fig 14) but the interference with the multi beam echo sounder in deep water implied that the ping rate used was lower than optimal.

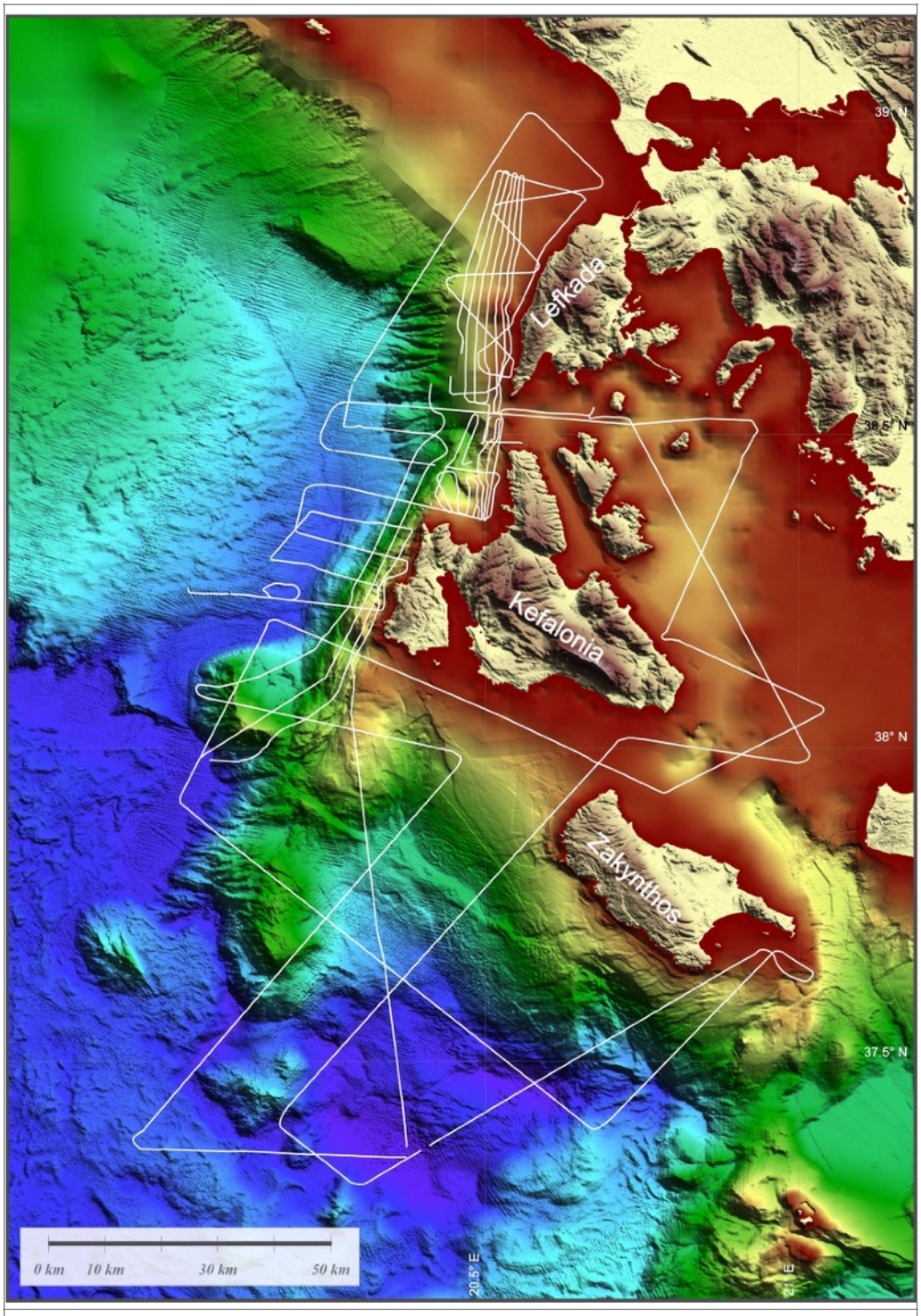

Figure 14: Map from all parasound data collected during POSEIDON cruise.

Sub-bottom chirp profiles were acquired using Topas PS18 (Kongsberg - Geoacoustic) with primary frequency in a range of 15-21 kHz, beam steering of 80° across and 20° along acquisition track.

The Chirp profiler shoot every 38 m in order to avoid frequency conflict with the multibeam system EM304. Their synchronized acquisition has been done using the k-sync system (Kongsberg Maritime). Obviously, the decrease in the shooting rate also decreases the spatial resolution of the records.

The images are however of good quality and we have chosen 4 segments from different areas to display examples of the variability of shallow features from a dynamic environment like the Ionian Islands tectonic setting.

Figure 15A displays the northern part of the basin located to east of Lefkada and Kefalonia islands (Figure 14). Shallow sediment is well-stratified and shows deformation associated to probable extensional faults in the western part and a gentle anticline in the eastern part. In the middle some ridges are present likely linked to the presence of Messinian evaporite.

Figure 15B shows one or two mass-transport deposit (MTD, the transparent body) covered by draping sediments above. The units underneath display changing reflectivity, are well-stratified an unconformable with the overlaying layering.

Figure 15C displays the steep escarpment associated to Kefalonia fault, west of the island (Figure 14). The seafloor and underlaying layers are characterized by a steep slope starved of sediment, as suggested by the low penetration of seismic energy. At the base of the slope there is a layer of sediments with internal deformations likely to be associated with a landslide of bodies moving down from the fault scarp.

Figure 15D shows an area characterized by the presence of a channel, here several sand waves and channel deposits lie above a fairly well stratified and undeformed sedimentary layer.

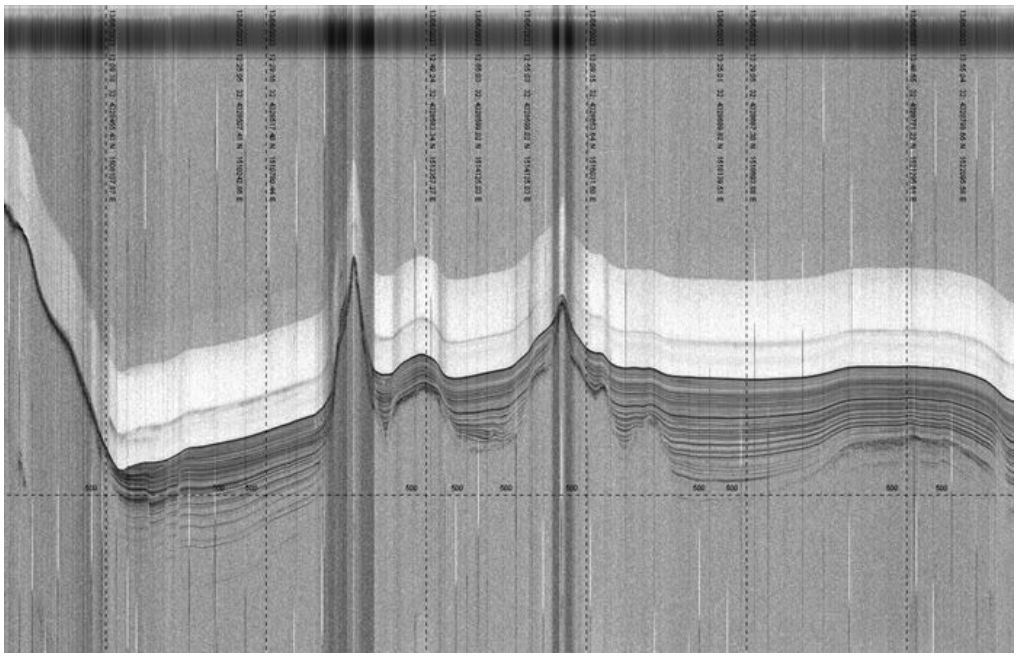

West East

A

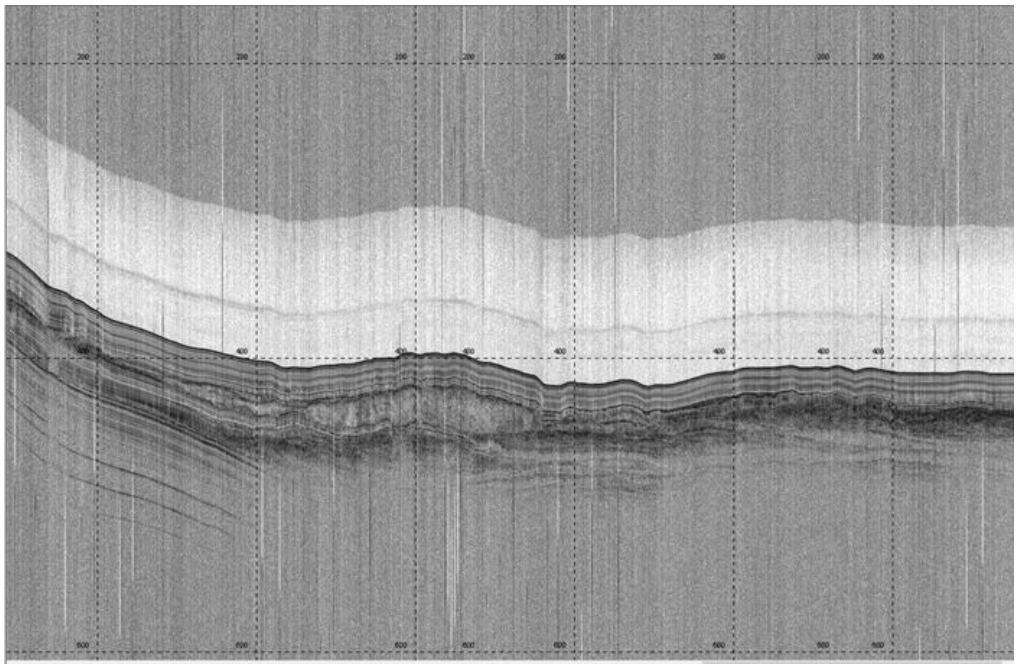

West East

B

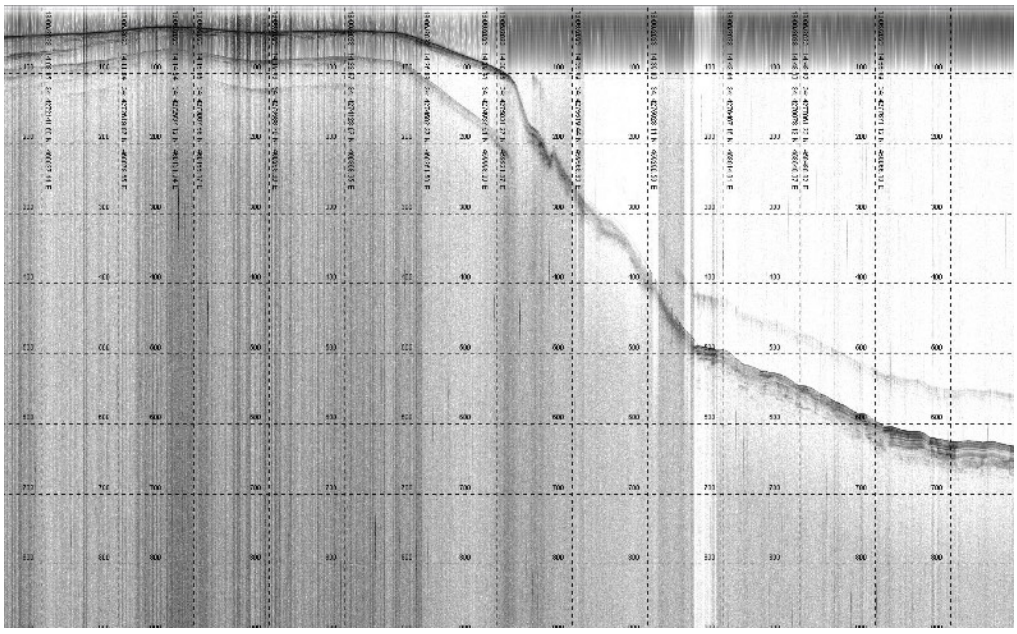

C

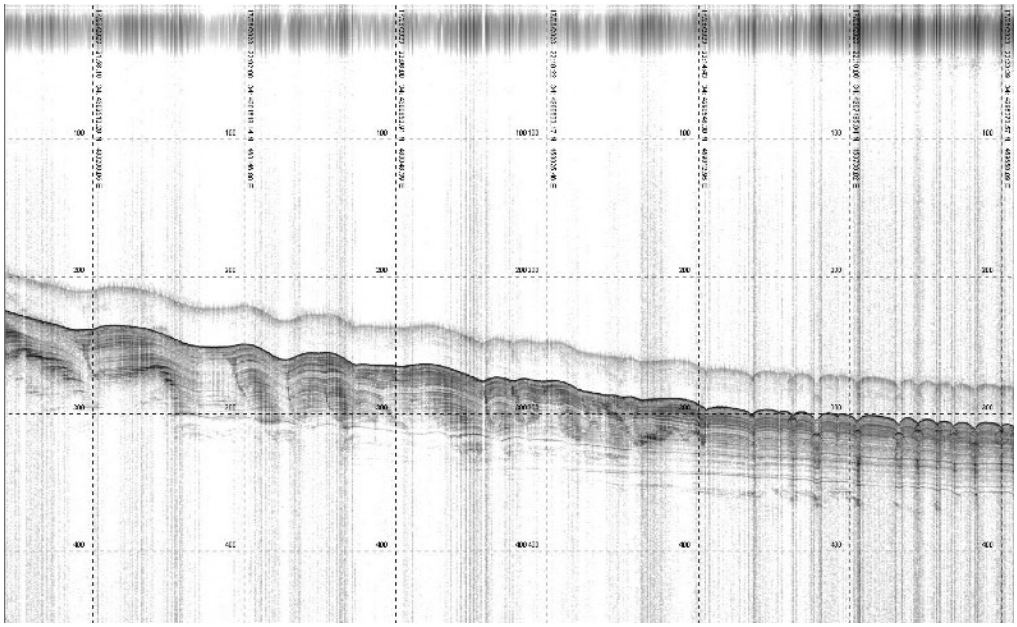

D

Figure 15: Four examples of Parasound data collected during POSEIDON. Description in the text.

6. SEDIMENT CORING

Sediment coring was positioned in two deep turbidite basins based on the seismic reflection images processed onboard. The basins are not interconnected and they seem to be fed by different submarine canyon systems so that turbidite synchrony could indicate regional events.

Figure 16: Gravity corer onboard R/V Laura Bassi being deployed during POSEIDON .

CORING LOG

Objectives: turbidites in deep basin Date: 19/06/2023

Sample Name: POSEIDON_23_GC-01

Latitude (°): 37° 58.846622' N

Longitudine (°): 20° 02.591728' E

	Date	UTC	Latitude	Longitude	Depth (m)
Corer at sea	19/06/23	14:42	37° 58.846694 N	20° 02.591667 E	
Corer at sea bottom	19/06/23	15:40	37° 58.846622' N	20° 02.591728' E	3695 m
Corer on board	19/06/23	16:24			

Penetration: 3,10 m *Recovered*: 2,2 m
Liner: 6 m
Sections: I (1 m)
II (1 m)
III (0,2 m)

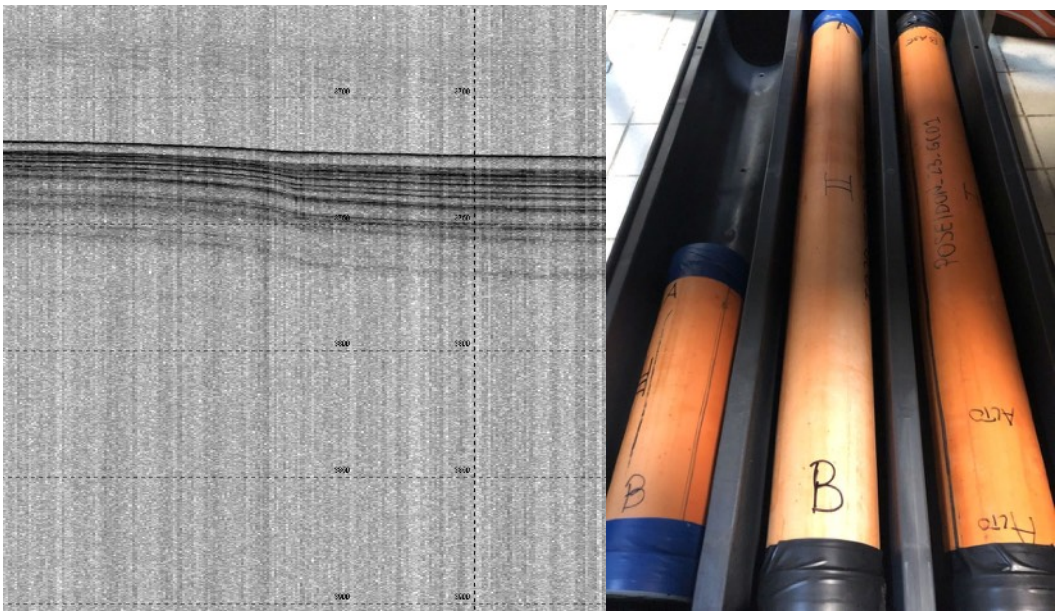

Fig 17. left: Topas image of the area where coring has been performed. On the right photos of core sections.

CORING LOG

Objectives: turbidites in deep basin Date: 20/06/2023

Sample Name: POSEIDON_23_GC-02

Latitude (°): 37° 20.788004’ N

Longitudine (°):20°22.572758’ E

	Date	UTC	Latitude	Longitude	Depth (m)
Corer at sea	20/06/23	08:12	37°20.787930’ N	20°22.572913’ E	
Corer at sea bottom	20/06/23	09:41	37° 20.788004’ N	20°22.572758’ E	4221 m
Corer on board	20/06/23	13:42			

Penetration: 3 m Recovered: 2,7 m + nose
Liner: 3 m
Sections:

Nose (0,1m)
I (1 m)
II (1 m)
III (0,7 m)

Notes: Technical problem. An overheating of the pulley, due to the frictional heat generated by the cable, blocked the cable. A second pulley it has been added to the system in order to recover the core.

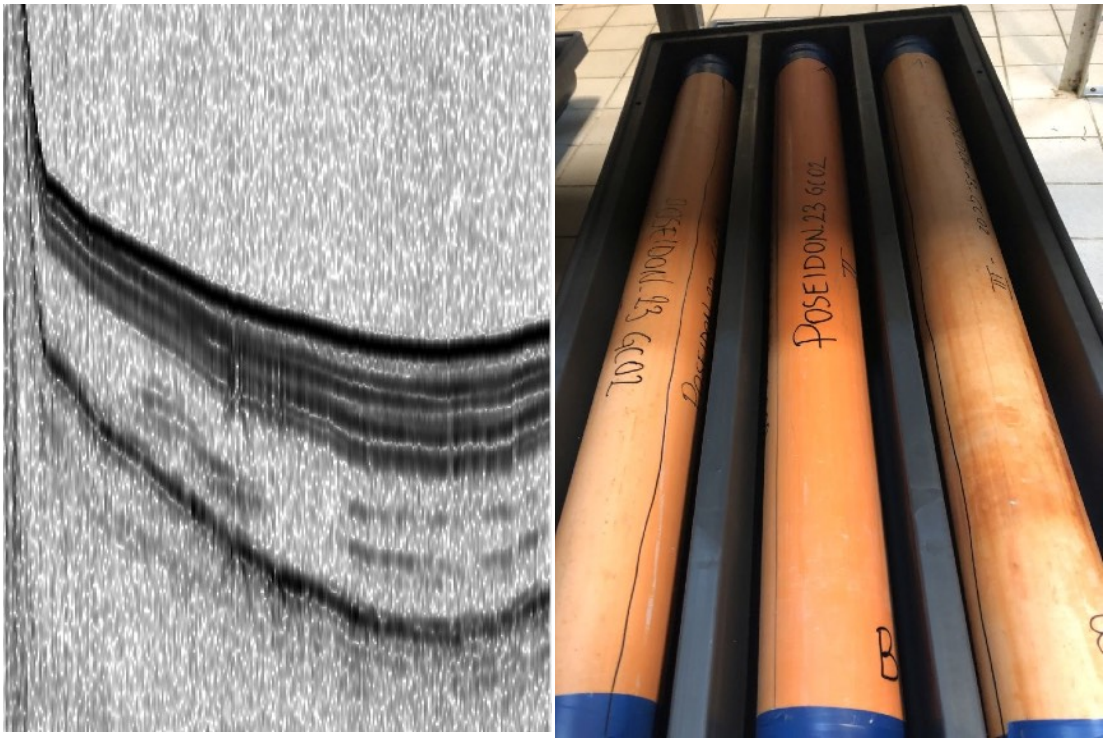

Figure 18: left: Topas image of the area where coring has been performed. On the right photos of core sections.

References

Cirella, A., et al.,. The 2018 Mw 6.8 zakynthos (Ionian Sea, Greece) Earthquake: Seismic source and local tsunami characterization, Geophys. J. Int. (2020).

Chousianitis, K., & Konca, A. O., Intraslab deformation and rupture of the entire subducting crust during the 25 October 2018 Mw 6.8 Zakynthos earthquake. Geophys. Res. Let., (2019)

Fujiwara, T. et al. The 2011 Tohoku-Oki earthquake: displacement reaching the trench axis. *Science* 2011.

Ganas, A., et al., Coseismic deformation, field observations and seismic fault of the 17 November 2015 M = 6.5, Lefkada Island, Greece earthquake, Tectonophysics, (2016).

Gómez de la Peña, L., Ranero, C.R., Gràcia, E. & Booth-Rea, G., Azañón, J.M., Tinivella, U., Yelles-Chaouche, A. Evidence for a developing plate boundary in the western Mediterranean. Nature Comm. 13. 4786. 10.1038/s41467-022-31895-z. (2022)

Govers, R. & Wortel, M. Lithosphere tearing at STEP faults: Response to edges of subduction zones. Earth Planet. Sci. Letters. (2005)

Gràcia E., et al. Ranero, C.R., Earthquake crisis unveils the growth of an incipient continental fault system. *Nature Comm.* (2019)

Haddad, A., Ganas, A., Kassaras, I., Lupi, M., Seismicity and geodynamics of western Peloponnese and central Ionian Islands: Insights from a local seismic deployment, Tectonophys., (2020)

Hansen, S. E., et al., Imaging slab detachment within the Western Hellenic Subduction Zone. G-3, (2019)

Herrendörfer R, et al., Earthquake supercycle in subduction zones controlled by the width of the seismogenic zone. *Nature Geoscience*, (2015).

Hore, H., A Forgotten European Disaster: The Great Cephalonia Earthquake 1953. Pages 17-19, GA Post-16 and HE Phase Committee. (2019)

Ilieva, M., P. Briole, A. Ganas, D. et al., Fault plane modelling of the 2003 August 14 Lefkada Island (Greece) earthquake based on the analysis of ENVISAT SAR interferograms, Tectonoph. (2016).

Karastathis, V. K., Mouzakiotis, E., Ganas, A. & G. A. Papadopoulos, High-precision relocation of seismic sequences above a dipping Moho: the case of the January–February 2014 seismic sequence on Cephalonia island (Greece) Solid Earth, (2015)

Maksymowicz, A. et al. Coseismic seafloor deformation in the trench region during the M_W8.8 Maule megathrust earthquake. *Scientific Rep.* (2017)

Lange, D. Et al. Interseismic strain build-up on the submarine North Anatolian Fault offshore Istanbul. Nature Comm. (2019)

Lay, T. et al. The great Sumatra–Andaman earthquake of 26 December 2004. *Science* (2005)

Lay, T. et al. Depth-varying rupture properties of subduction zone megathrust faults. *J. Geophys. Res*. 117, B04311 (2012).

Noda, H. & Lapusta, N. Stable creeping fault segments can become destructive as a result of dynamic weakening. *Nature* 518–521 (2013)

Özbakir, Ali Değer, Evolving plate boundaries in the Aegean–Anatolian region. Utrecht Studies in Earth Sciences, volume 199 (PhD Dissertation) 2019.

Pearce, F. D., et al. Seismic investigation of the transition from continental to oceanic subduction along the western Hellenic subduction zone. *J. Geophys. Res.* (2012)

Pérouse, E., N. et al., Bridging onshore and offshore present-day kinematics of central and eastern Mediterranean: Implications for crustal dynamics and mantle flow, G-cubed (2012)

Piana Agostinetti, N., et al., Across-fault velocity gradients and slip behavior of the San Andreas Fault near Parkfield. Geoph. Res. Let. 4 (2020)

Saltogianni, V., et al., The 2014 Cephalonia Earthquakes: Finite Fault Modeling, Fault Segmentation, Shear and Thrusting at the NW Aegean Arc (Greece), *Pure Appl. Geophys*. (2018)

Saranga, D. '60 Years Ago This Month', www.huffingtonpost.com/david-saranga/60-years-ago-this- month_b_3759560.html?guccounter=1 (2017)

Stiros, S.C., et al. The 1953 earthquake in Cephalonia (western Hellenic arc): coastal uplift and halotectonic faulting. *Geophys. J. Int*. (1994)

Sun, T., et al., Large fault slip peaking at trench in the 2011 Tohoku-Oki earthquake. *Nature Comm.* (2017)

Underhill, J. R. Late Cenozoic deformation of the Hellenide foreland, western Greece. Geological Soc. America Bulletin, 101, 613–634. (1989)

Underhill, J. R. Relocating Odysseus' homeland. Nature Geoscience, 2, 455-458 (2009).

ANNEXES

ANNEX A

VESSEL'S CHARACTERISTICS

R/V LAURA BASSI	
Yard	Kverner Kleven Leirvik, Norway
Built	1995
Flag	Italy
Call sign	ZDLS1
IMO No.	9114256
Owner	National institute of Oceanography and Applied Geophysics - OGS
Operator	Argo Diamar

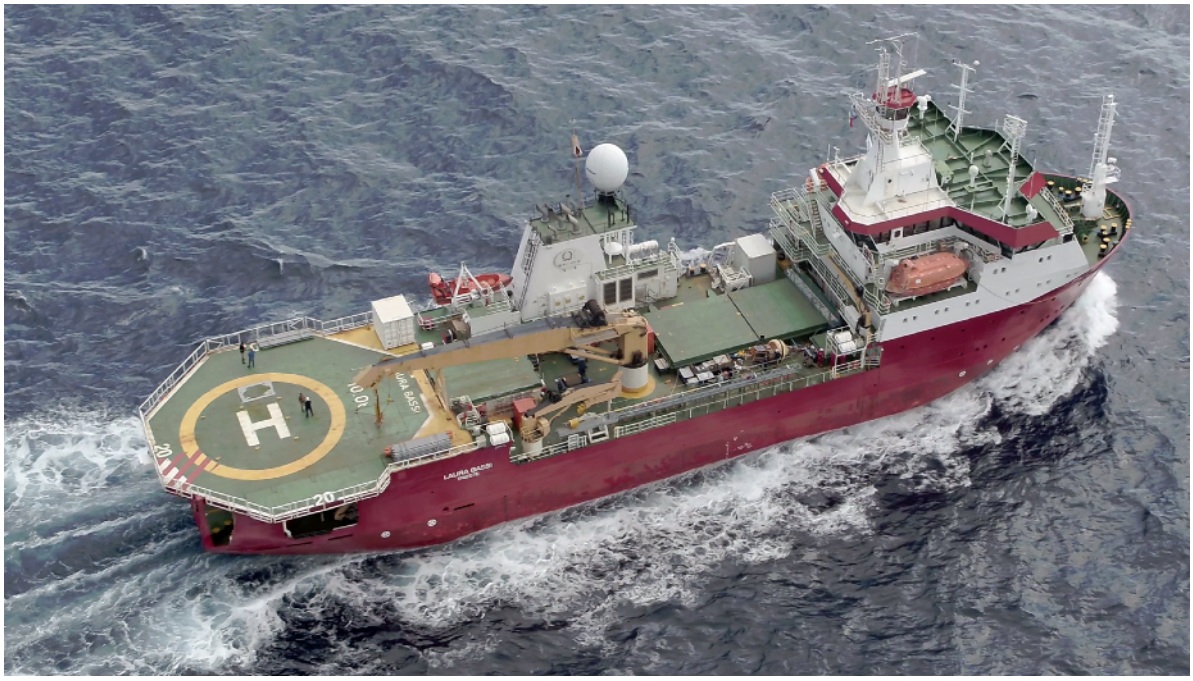

Aerial view of the research vessel Laura Bassi

General Arrangement

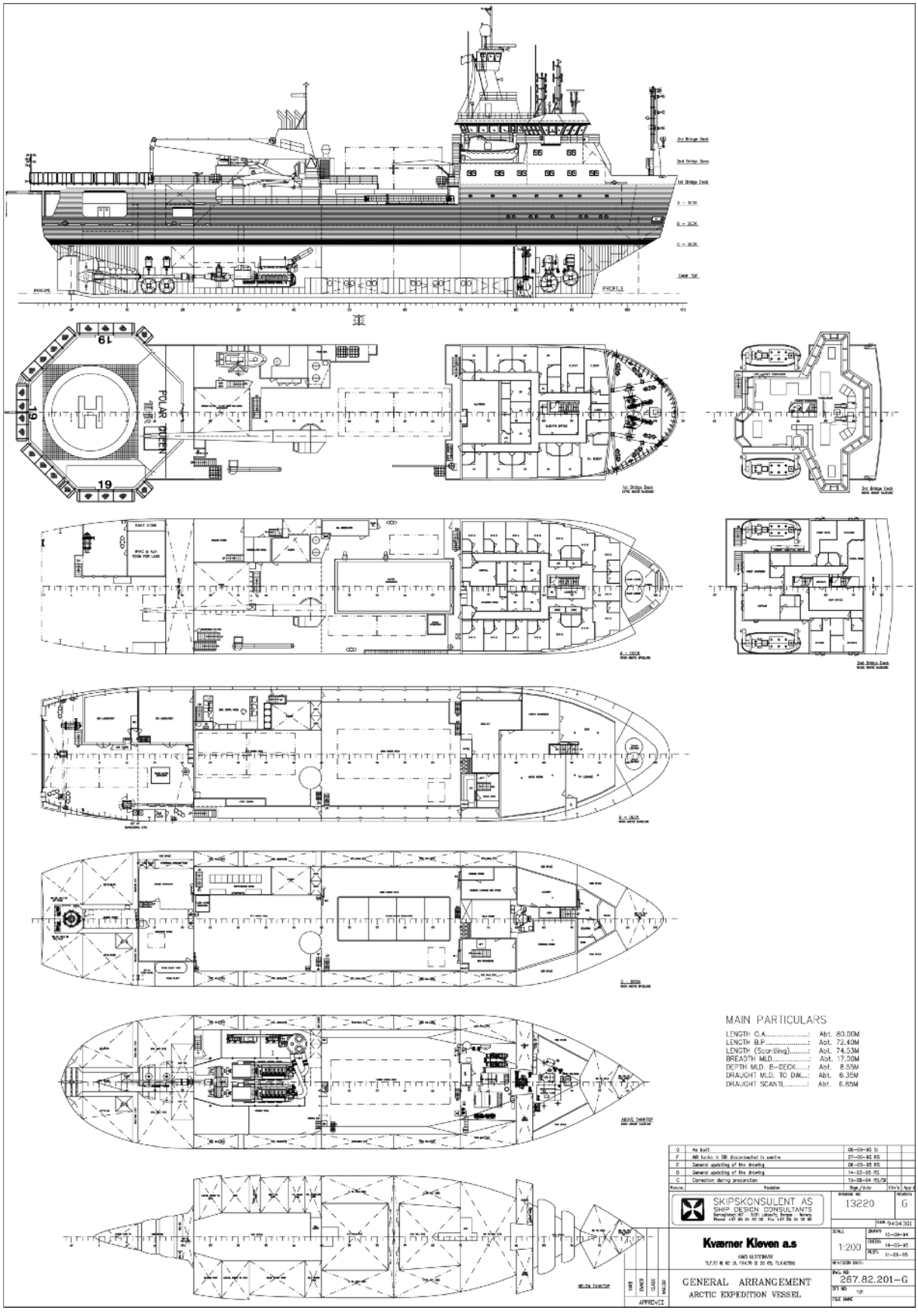

CLASS NOTATION

RINa C ✠
special service - research ship - unrestricted
✠ AUT-UMS; ✠ DYNAPOS DP2 ; HELIDECK
ICE CLASS IA; WINTERIZATION (temp -30 °C)

PRINCIPAL DIMENSIONS

Length O.A.	80.00 m
Length B.P.	72.40 m
Breadth mld.	17.00 m
Depth mld. (to B-	8.55 m
Draught Scantl.	6.85 m
DWT	1910 tonnes
GRT	4028
Port of registry - No	Trieste - 807

CAPACITIES

Fuel Oil	1250 m^3
Fresh Water	165 m^3
Kerosene (Jet A1)	160 m^3

MACHINERY AND PROPULSION

Main Engines

Make	Bergen Diesel
Type	BRG 6
Rated Power	2 x 2280 kW @ 720 rpm

Main propulsion

C/P Propeller:	1 o# in Nozzle
Make	Ulstein
Blades	4
Bollard pull	100% pitch - 75 tonnes
	75% pitch - 62 tonnes
	50% pitch - 44 tonnes

Auxiliary Engines

Make	Mitsubishi
Type	S6R-MPTK
Rated Power	2 x 590 kW/1800 rpm

THRUSTERS

Bowthruster 1	600 kW
Bowthruster 2	800 kW
Azimuth fwd	800 kW (retractable)
Sternthruster 1	600 kW
Sternthruster 2	600 kW

ROLL REDUCTION

2 x integrated roll reduction tanks

HIGHLIGHTS FOR CHARTERER'S SPECIAL USE

Water supply:

• Uncontaminated sea water supply

• Freshwater production: 2 x 25m3 Fresh Water Production

Hydraulic Power Pack:

• 2 x 120 ltr/min – 210 Bar, outlets in cargo holds and on deck

Gate Valve:

• DN400 (16") in fwd HPR trunk

Utility SWB:

Utility SWB's in engine work shop

Utility SWB no1, 450V - 630 A / Conn. 2 x 100A, 2 x 250A and 1 x

Utility SWB no2, 450V - 630 A / Conn. 2 x 100A, 1 x 250A and 1 x

Distribution boxes in cargo holds and aft deck:

Total 450 V - 320A (each box 160 A)

Total 230 V - 160A (each box 160 A)

ELECTRICAL PLANT

Shaft Generators

Make	AVK
Rating	2 x 2 200 kW

Auxiliary Generators

Make	Mitsubishi
Rating	2 x 590 kW

Emergency Generators

Make	Mitsubishi - AVK
Rating	1 x 152 kW, 3 x 450 V, 60 Hz

Emergency generator

El. Distribution

440 V, 230 V and 110 V all 60 Hz

WORKSPACE AND DECK AREAS

Tank top:	
Distributed load	5.3 t/m2
Container loads	3 tiers 20 TEU max stack weight 72 t
Cargo handling vehicles with max axle load 15 t and single pneumatic tyres.	

C-Deck cargo area:	
Distributed load:	1.65 t/m2
Cargo handling vehicles with max axle load 15 t and single pneumatic tyres	

B-Deck aft deck	
Distributed load	5.0 t/m2

A-Deck	
Distributed load	1.65 t/m2
Container loads	1 tiers 20 TEU max weight 24t
Cargo handling vehicles with max axle load 15 t and single pneumatic tyres	

DECK EQUIPMENT

Main Crane

Maker:	Norlift
Type	GPCO 900 – 5020 straight boom
Design	LRS, Ch. 3 Section 2
Specification	

Capacity	Outreach	Seastate	Fall	Hook speed loaded	Hook travel
50t	20m	NA	Four	8 m/min	62m
50t	10m	1	Four	8 m/min	62m

Provision crane

Maker	Norlift
Type	GP
Specifcation	2 t / 7 m

Aft deck crane

Maker	Norlift
Type	Telescopic boom
Specifcation	10 t / 5m
Winch capacity	2.75t
hook travel	15 m

Hatches

A-deck	14 x 6 m
B-deck	14 x 5.4 m (flush)
Helideck	7 x 6 m (flush)

HELIDECK

D-Value	19.5 m
Make take off and landing wight	Designed for Super Puma

MANOEUVRING, NAVIGATION AND COMMUNICATION

Dynamic Position System:

- Kongsberg K-Pos 21 + CJOY Remote Joystick
- Simrad LTW MK 8-15S Modified (500m)
- Seatex Seapath 200
- Seatex DPS 132
- STARFIX RTCM Correction Receiver
- MBX-4 IALA RTCM Correction Receiver

50t	8.4m	2-3	Four	8 m/min	62m
34t	8.4m	5-6	Four	8 m/min	62m
25t	20m	-	Two	16 m/min	125m
12.5t	21m	5-6	Single	32 m/min	250m
Aux 5t	19m	NA	Single	60 m/min	40m

Work Crane

Maker	Norlift
Type	GPFO 160 – 0510 folded jib crane
Design	LRS, Ch. 3 Section 2
Specification	

Capacity	Outreach	Seastate	Hook speed empty	Hook speed loaded	Hook travel
5t	10m	6	90m/m	37m/min	35m

- MDL Fanbeam MK 4.2 Position Sensor
- HPR HiPAP 501
- HPR 410 Standard
- Interface to APos System
- Interface to DGPS NO.2
- 3 x Seatex MRU-5
- 3 x Anschutz Gyro
- Serial NMEA outputs Available
- Dief Wind Sensor Anemometer – 879
- 2 x Gill Sonic DP Wind Sensor
- Rudder, Thruster & Propulsion Control
- Propulsion Control
- Rudder Control
- Thruster Control
- ERN 99, 99, 96

Navigation

Integrated Bridge System – Kelvin Hughes IBS Paperless Bridge

- Kelvin Hughes IBS
- Kelvin Hughes - X Band Manta Digital Radar
- Kelvin Hughes - S Band Sharpeye Radar
- Kelvin Hughes MDP-A2-ABAA ECDIS System (not certified)
- Bridge Watch Monitoring System
- 3 x Anschutz STD 20 Gyros
- Skipper GDS 101 Echo Sounder
- Kelvin Hughes MDP-A1 Slave radar
- Furuno Doppler Current indicator CI-600G
- Kelvin Hughes MDP-A2 Route Planning Station
- DGPS 1 - Furuno GPS90 GPS/ Seatex DPS 123
- DGPS 2 - Seatex Seapath 200
- Kelvin Hughes SEM 200 Autopilot
- Sperry Naviknot 350 E Speed Log
- Seatex HMS 100 Helicopter Motion and Weather
- Helicopter Transponding System
- Maneuvering Joystick System: Ulstein PosCon
- Navigation Information Network - ADB / LAN

1 X Becker Rudder Tenfjord Steering gear

Scientific Bridge Equipment

- Simrad EA 600 Hydrographic Echo Sounder
- AME 2006 Shipbourne Three Component Magnetometer
- Automatic Weather Reporting Station
- UK Meteorological Measuring Equipment

Navigation Information Network

LAN: 4 access CISCO switch working at ISO/OSI level 2

1 CISCO switch level 3 + 1 Palo Alto Firewall

WIFI: 6 access point - one for each bridge and in the dry lab.

COMMUNICATION

Communication and Radio Equipment including GMDSS for Area 4

- Console N
- HF Radio 2
- Taiyo Auto RDF
- Watch Receiver
- Weather Fax
- Console Q1
- Sailor Inmarsat C - LRIT Compliant
- HF Radio 1
- Console Q2
- Console C
- VHF No. 1
- Console A
- Broadgate S-VDR
- Console G
- Kelvin Hughes UAIS
- Console R2
- VHF No. 2
- Console R3
- VHF No.3
- Helicopter Beacon
- Areonautical VHF
- Console M
- LP2 Domestic Supply
- EMP2 Emergency Switchboard Supply
- UPL1 Eaton 3KVA MKV
- UPL2 Eaton 3KVA MK
- Immarsat Fleet 77 Satellite Communications
- VSAT C-band Satellite Communications
- Iridium Certus Satellite Communications
- Immarsat FleetBB Satellite Communications (Optional)

ACCOMODATION

High standard accommodation comprising facilities such as: Reception area, ships office, change room, recreation area, trim room, sauna, mess, TV/Crew dayroom, charterer's lounge, launderettes, laundry, client office
Crew: 24 berths
Available for charterers
2 single client rep. cabin = 2
4 cabins x 2 berths = 8
9 cabins x 3 berths = 27
6 cabins x 4 berths = 24
Total 61 berths
All cabins with toilet and shower
Hospital: 1 berth

LIFESAVING AND RESCUE EQUIPMENT

Lifesaving and rescue equipment according to SOLAS	
Life boats: 2 x Harding MCB24CR - 40 persons	
Life boat davits: 2 x Vestdavit H-7000	
M.O.B. Boat: 1 x Norsafe Magnum 7.5	
M.O.B. Boat davit: 1 x Vest Davit P-3000, with shock damper.	
Life rafts: 8 x RFD (each 20 men).	
Survival suits: 80 off	
Lifejackets: 80 off	
EEBD's: 6 off	
Smoke Hoods: 38 o# (2 per SPP Cabin)	
Fire Extinguishing:	
Accommodation	Flexifog Fixed Fire
	Dampening System
	CO2, Dry Powder and AFF Extinguishers
Galley, Paint store, and Sw Board	CO2
Cargo Holds	AFF Hi Ex Foam
Engine Room	AFF Hi Ex Foam
Helideck	AFF Low Ex Foam

VESSEL'S OFFSETS

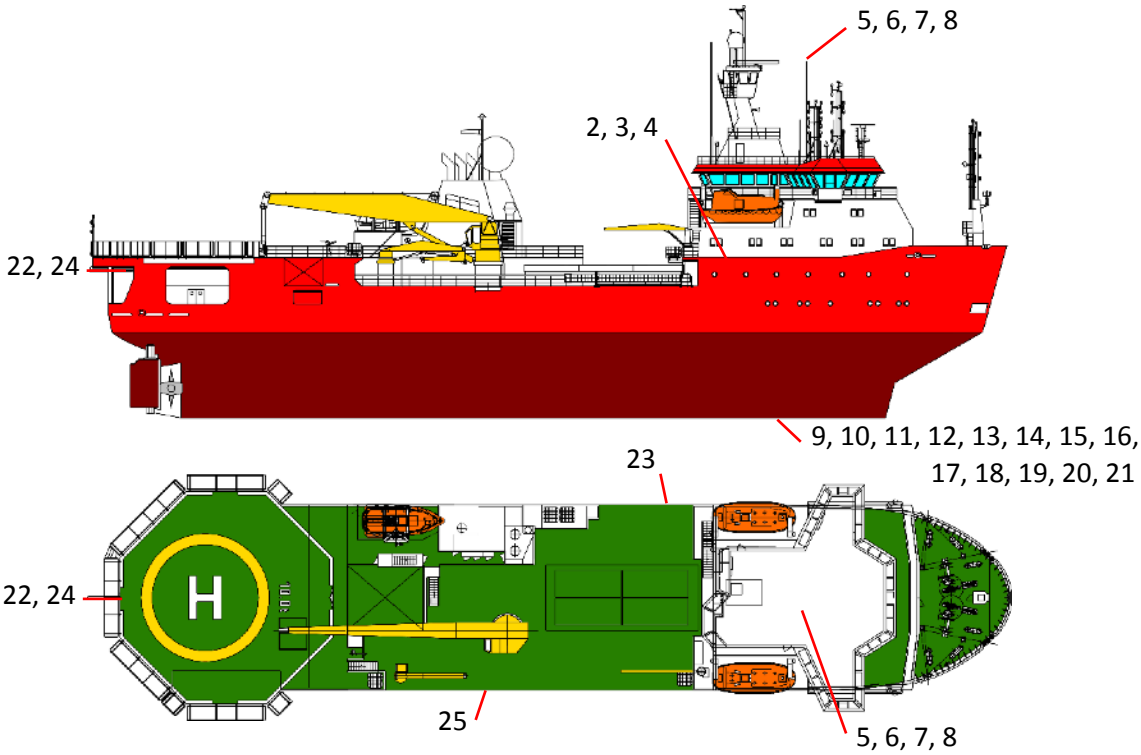

#	Equipment	x	y	z
1	Zero offset	0.000	0.000	0.000
2	MRU1	-0.375	0.025	0.103
3	MRU2	0.279	0.029	-0.043
4	MRU3	0.739	0.047	0.100
5	SEAPATH200 bow	1.992	2.861	29.006
6	SEAPATH200 stern	1.914	0.354	28.953
7	SEAPATH380 bow	2.053	3.612	28.945
8	SEAPATH380 stern	1.925	-0.405	28.861
9	EM2040	0.574	-0.767	-7.978
10	TX EM304	2.777	0.828	-7.433
11	RX EM304	1.624	3.628	-7.420
12	EK80 18 kHz	1.614	-1.729	-7.443
13	EK80 38 kHz	1.613	-3.501	-7.471
14	EK80 70 kHz	1.416	-2.385	-7.495
15	EK80 120 kHz	1.832	-2.915	-7.501
16	EK80 200 kHz	1.865	-2.387	-7.502

SIGN CONVENTION

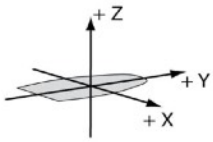

17	EK80 333 kHz	1.393	-2.916	-7.504
18	TOPAS	0.899	1.878	-7.407
19	EA600	1.614	-0.326	-7.442
20	ADCP 150 kHz	1.771	0.4820	-7.495
21	ADCP 38 kHz	2.763	-1.969	-7.481
22	STERN	0.000	-54.200	-
23	SVP 1	8.400	-35.000	-
24	SVP 2	0.000	-54.200	-
25	CORING	10.000	-15.000	-

ANNEX B

SCIENTIFIC EQUIPMENT

ACOUSTICS SYSTEMS

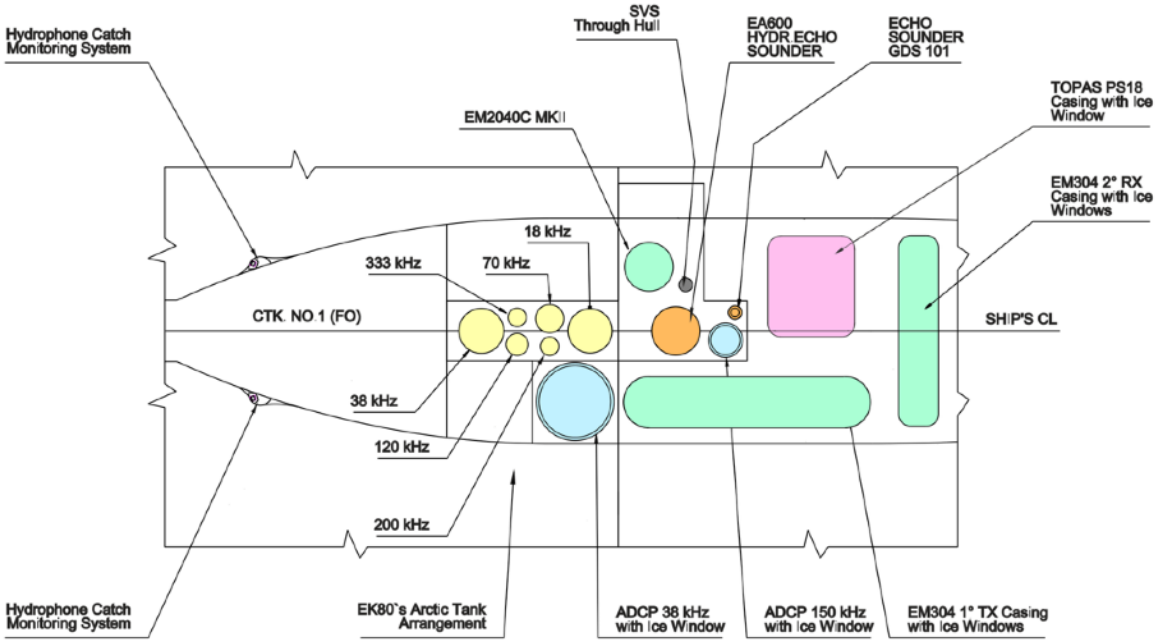

Top: Plan view of the view of the keel block where the transducers are hosted. In yellow the scientific equipment; in orange the ship echosunders.

Bottom right: the keel after the installation of the transducers was completed.

Bottom left: 3D model of the block

ACOUSTIC SYSTEMS SINCHRONIZATION

Equipment	Sinchronizing Unit			
Manufacturer	Kongsberg Maritime			
Model	K-Sync			
Installation	Rack mounted			
Max No. of systems	16			
Trigger period calculation	From external depth			
List of controlled equipment	Type	Model	Frequency range (KHz)	Group
	SBES	EK80	18-38-70-120-200-333	2
	MBES	EM2040	200-400	1
	MBES	EM304	26-34	1
	SBP	TOPAS PS18	1-6	3
	ADCP	OS 150	150	1
	ADCP	OS 18	38	4

MORPHOBATYMETRY – DEEP WATER	
Equipment	Multibeam echosounder
Manufacturer	Kongsberg
Model	EM 304
Installation	Keel mounted
Nominal frequency	30 KHz
Operating frequency	26-34 KHz
Swath width	Typically 5.5 times the depth, or more than 9 km
Number of swath	2 swaths per ping
Pulse length	0.4 ms CW to 200 ms FM effective pulse length
Number of transmit sectors	16 frequency coded transmit sectors per ping / 8 per
Available models	0.5 degree, 1 degree, 2 degrees and 4 degrees
Number of receiver beams (per ping)	1600 beams, 0.5 degree RX and 1 degree RX 1024 beams, 2 degree RX 512 beams, 4 degree RX
Beam focusing	On transmit and receive
Realtime motion stabilization	Roll: ± 15 ° Pitch: ± 15 ° Yaw: ± 15 °
Sounding pattern	Equidistant and equiangular
Gain control	Automatic
Mammal protection	Gradual start up transmit ramp
Deliverables	Bathymetric data Seabed imagery data Water column data Extra depth detections

MORPHOBATYMETRY – SHALLOW WATER	
Equipment	Multibeam echosounder
Manufacturer	Kongsberg
Model	EM 2040c MKII
Installation	Drop pole mounted
Frequency range	200 to 400 kHz in steps of 10 Hz
Beam width	1° x 1 ° at 400 kHz
Max ping rate	50 Hz
Swath coverage	Up to 140° (5.5 times water depth)
Beam patterns	Equiangular, equidistant and high density
No. of beams per ping	400
Roll stabilized beams	± 15°
Pitch stabilized beams	± 10°
Yaw stabilized beams	± 10°
Depth range	Up to 520 m at 200 kHz
Pulse type	Continuous Wave (CW) / Frequency Modulated (FM – chirp)
Pulse lengths	
CW	14, 27,54, 135, 324 and 918 µ
FM	3 and 12 ms
Water columns logging	Yes

SUB BOTTOM PROFILING	
Equipment	Sub bottom profiler
Manufacturer	Kongsberg - Geoacoustic
Model	Topas PS18
Installation	Keel mounted
Primary frequency	15-21 KHz
Secondary frequency	5. – 6 KHz
Output power	>32 KW
Beamwidth primary	~3.5°
Beamwidth secondary	~4.5° x 4.5°
Source level	~209 dB ref. to 1 µPa@1m
Dynamic range	>110 dB
Range resolution	<0.15 m
Available pulse types	Continuous Wave (CW), Ricker, Frequency Modulated (FM
Depth range	<20 - >11000m
Beam steering	80° across / 20° along
Navigation input	NMEA 0183 (UDP)
Depth / slope input	NMEA 0183 (UDP)
Real time processing	TVG, Digital band pass filter, Deconvolution, Matching filters, etc.
Synchronization unit	K-sync

PHYSICAL OCEANOGRAPHY – ACOUSTIC DOPPLER CURRENT PROFILER

Equipment		Acoutic Doppler Current Profiler - ADC				
Manufacturer		Teledyne RD Instruments (TRDI)				
Model		Ocean Observer III				
Installation		Keell mounted				
No. of transducers		2				
Model		Ocean Surveyor				
			38 KHz		150 KHz	
		Vertical res. cell size	Max	Precision	Max Range	Precision
Water Profiling	Long Range Mode	4			>350 m	30 cm/s
		8			>400 m	16 cm/s
		16	>1000 m	30 cm/s		
		24	>1000 m	20 cm/s		
	High Precision Mode	4			>225 m	15 cm/s
		8			>250 m	8 cm/s
		16	>900 m	15 cm/s		
		24	>950 m	10 cm/s		
Profile Parameters		Velocity Accuracy	± 1% ± 0.5 cm/s		± 1% ± 0.5 cm/s	
		Velocity range	-5 to 9 m/s		-5 to 9 m/s	
		Number of depth	1-128		1-128	
		Max ping rate	0.4 m		1.5 Hz	
Echo intensity Profile		Vertical Resolution	Depth cell size, configurable			
		Dynamic Range	80 dB			
		Precision	±1.5 dB			
System power		Power	1400 W			
Transducer		Bean angle	30°			
		Configuration	4-beam, phased array			

SEABED SAMPLING

Equipment	OSIL piston corer operating with trigger-arm
Maximum core length	15 m using 3 m and 5 m long barrels
Barrel diameter (ID-OD)	102 mm Inner Diameter and 114 mm Outer Diameter
Plastic liner OD	100 mm
Corer Head	300 kg, variable by adding/removing layers of lead weights
Trigger weight	100 kg
Trigger pilot (gravity core)	1 m long,
Total weight	1500 Kg
Winch	Ibercisa
Cable length	6000 m
Cable diameter	12 mm

ANNEX C
POSEIDON SEISMICS

SEISMIC ACQUISITION PARAMETERS

ACQUISITION PARAMETERS

Geodetic parameters

Acquisition datum	WGS84
Projection	UTM
Zone	34

Navigation system

Software	PDS2000

Source

Model	250 cu.in G.Gun
Array	4 x 250 G.Gun rectangular (2 m x 1 m)
Total volume	1000 cu.in.
Shot Interval	37.5 m
Towing depth	5 m

Synchronization

Model	Hot Shot Teledyne
Aiming point	50 ms (upward bulk static to be applied to raw data)

Recording

Model	Sercel Seal 428
Channel number	120
Channel distance	12.5 m
CDP distance	6.25 m
Sample rate	1 ms
Record length	12 s
Low cut filter	3 Hz
High cut filter	8N
Towing depth	7 m

Leveling System

Model	Digicourse SYS 3
Number of birds	7

ACQUISITION GEOMETRY

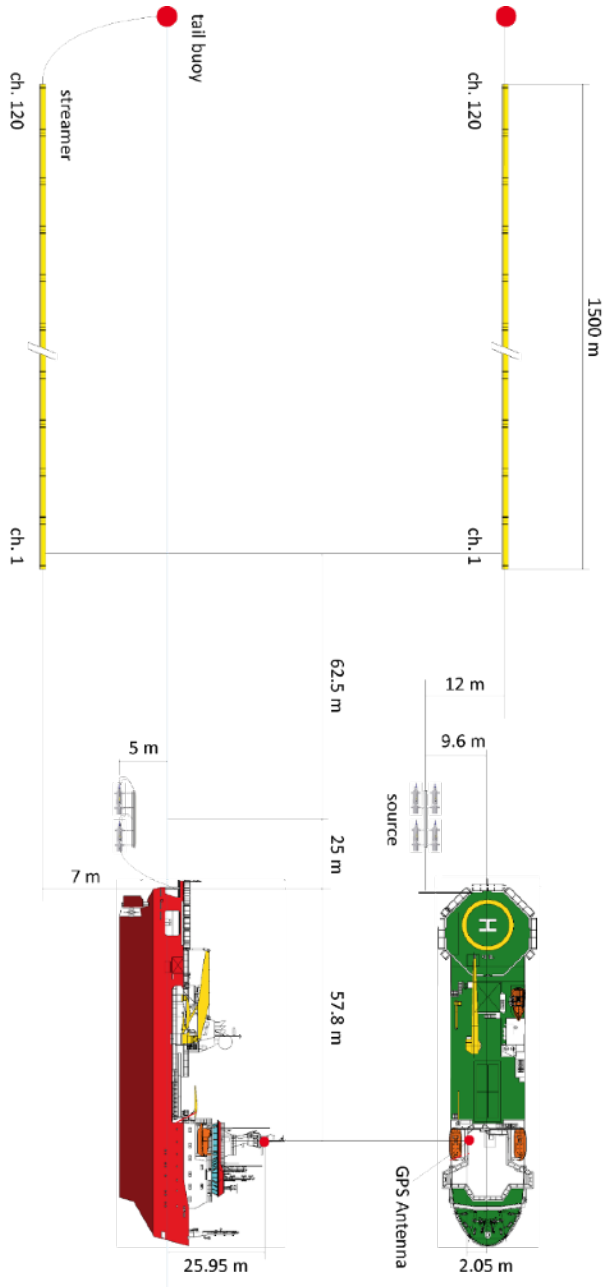

STREAMER and BIRDS CONFIGURATION

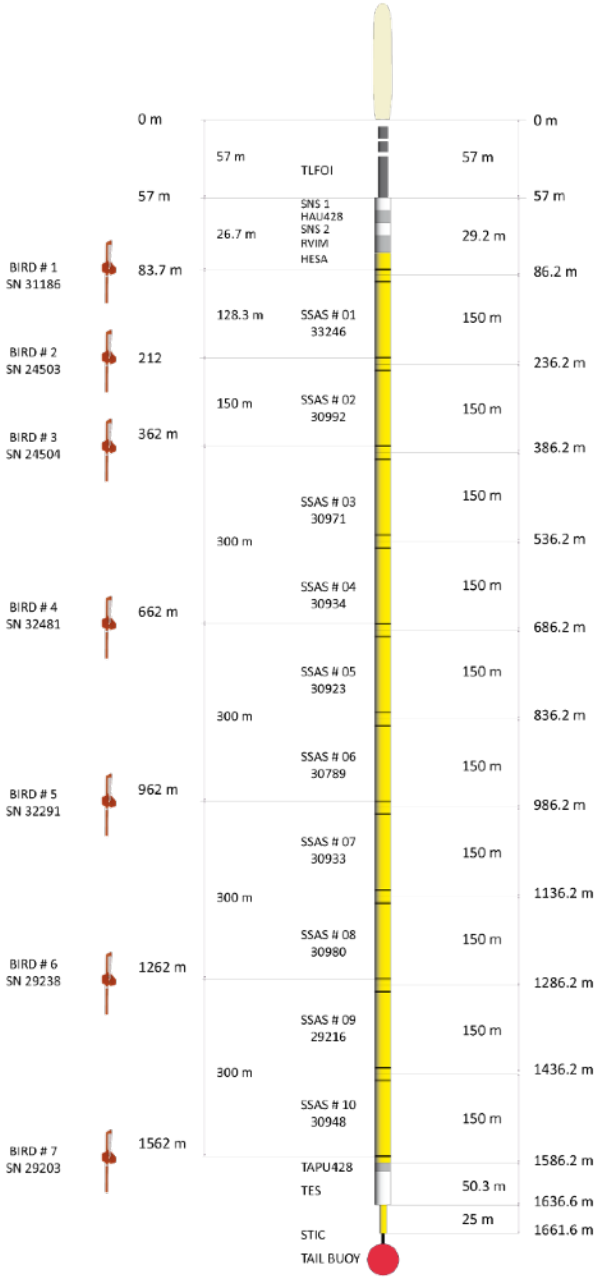

LINE CHANGING APPROACH

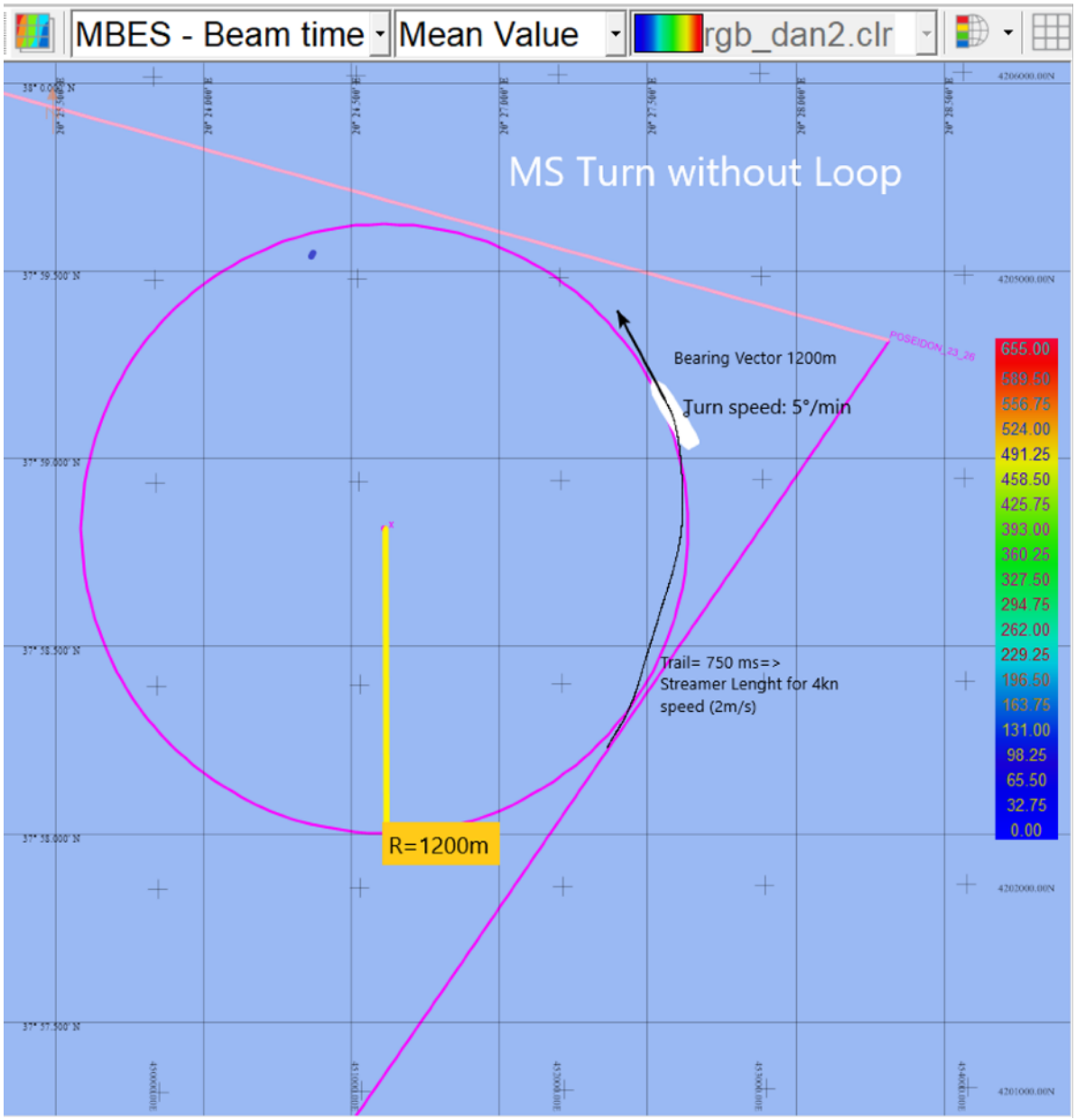

POSEIDON SEISMIC LINES PRODUCTION STATS

POSEIDON Seismic Profiles

Line Name		Date	Time	Duration	SP	SP TOT	Lon	Lat	X	Y	Distance
POSEIDON_23_01	SOL	6/12/23	20:47	1h 48m 35s 232ms	101	387	020°09.91283131'E	038°14.29579535'N	426945,161577	4232580,767414	14470,360968
	EOL	6/12/23	22:36		487		038°13.17707149'N	020°19.72910723'E	441247,905771	4230395,43931	
Line Name		Date	Time	Duration	SP	SP TOT	Lon	Lat	X	Y	Distance
POSEIDON_23_02	SOL	6/12/23	23:54	1:51	101	387	038°17.98544211'N	020°21.99005656'E	444607,37079	4239264,37068	14469,963980
	EOL	6/13/23	1:45		487		038°20.40408480'N	020°12.54614453'E	430882,67609	4243843,306474	
Line Name		Date	Time	Duration	SP	SP TOT	Lon	Lat	X	Y	Distance
POSEIDON_23_03	SOL	6/13/23	3:00	2h 58m 17s 610ms	101	617	038°25.17641582'N	020°14.25820900'E	433449,276503	4252648,091371	3093,93105354
	EOL	6/13/23	5:59		717		038°21.89348366'N	020°29.54179089'E	455652,45138	4246423,676018	
Line Name		Date	Time	Duration	SP	SP TOT	Lon	Lat	X	Y	Distance
POSEIDON_23_04	SOL	6/13/23	7:06	2h 47m 5s 200ms	101	585	038°26.31927645'N	020°30.43462914'E	456996,169153	4254601,445104	894,73046398
	EOL	6/13/23	9:54		685		038°28.41846294'N	020°15.62584329'E	435487,227584	4258627,653365	
Line Name		Date	Time	Duration	SP	SP TOT	Lon	Lat	X	Y	Distance
POSEIDON_23_05	SOL	6/13/23	11:08	7h 4m 15s 102ms	101	1493	038°33.06671986'N	020°16.72528950'E	437153,048435	4267211,445012	36046,893573
	EOL	6/13/23	18:13		1593		038°31.31956322'N	020°55.12690499'E	492920,0948	4263736,903	
Line Name		Date	Time	Duration	SP	SP TOT	Lon	Lat	X	Y	Distance
POSEIDON_23_06	SOL	6/13/23	18:40	4h 46m 51s 635ms	101	1005	038°29.79616805'N	020°55.68948950'E	493735,249604	4260918,913323	643,22363777
	EOL	6/13/23	23:27		1105		038°10.71383661'N	020°46.89257623'E	480866,642528	4225649,908534	
Line Name		Date	Time	Duration	SP	SP TOT	Lon	Lat	X	Y	Distance
POSEIDON_23_07	SOL	6/13/23	23:52	2:48	101	600	038°10.07900811'N	020°48.79316626'E	483638,636454	4224469,88221	459,58602558
	EOL	6/14/23	2:40		700		038°03.98590008'N	021°02.09011871'E	503055,686294	4213186,36606	
Line Name		Date	Time	Duration	SP	SP TOT	Lon	Lat	X	Y	Distance
POSEIDON_23_08	SOL	6/14/23	2:55	3h 11m 20s 569ms	103	671	038°03.09395384'N	021°01.83232526'E	502679,342524	4211536,828689	121,23601336
	EOL	6/14/23	6:06		773		037°55.77304581'N	020°47.37671397'E	481510,82004	4198019,443963	
Line Name		Date	Time	Duration	SP	SP TOT	Lon	Lat	X	Y	Distance
POSEIDON_23_09	SOL	6/14/23	6:20	7h 40m 45s 798ms	101	1628	037°56.00839727'N	020°46.22869167'E	479830,394731	4198458,619928	001,40103078
	EOL	6/14/23	14:00		1728		038°12.24168400'N	020°09.94293928'E	426954,851928	4228781,667346	

Line Name		Date	Time	Duration	SP	SP TOT	Lon	Lat	X	Y	Distance
POSEIDON_23_10	SOL	6/14/23	14:11	4h 8m 21s 283ms	101	878	038°11.95322653'N	020°09.15157911'E	425795,169522	4228258,701678	882,60513190
	EOL	6/14/23	18:19		978		037°55.43689631'N	020°00.84339904'E	413346,432714	4197835,23864	
Line Name		Date	Time	Duration	SP	SP TOT	Lon	Lat	X	Y	Distance
POSEIDON_23_11	SOL	6/14/23	18:29	10:18	101	2168	037°54.62957961'N	020°00.84870068'E	413338,411493	4196342,231819	206,73868591
	EOL	6/15/23	4:47		2268		037°23.63362991'N	020°39.98248509'E	470469,118605	4138621,962568	
Line Name		Date	Time	Duration	SP	SP TOT	Lon	Lat	X	Y	Distance
POSEIDON_23_12	SOL	6/15/23	5:04	4h 46m 41s 180ms	101	1002	037°23.97404152'N	020°41.34973761'E	472488,240119	4139244,500942	37529,75
	EOL	6/15/23	9:51		1102		037°39.93413891'N	020°57.08064693'E	495708,816564	4168711,373612	
Line Name		Date	Time	Duration	SP	SP TOT	Lon	Lat	X	Y	Distance
POSEIDON_23_13	SOL	6/15/23	12:14	9h 15m 25s 43ms	101	1962	037°39.40503927'N	020°57.86804010'E	496865,842229	4167732,498671	73403,49
	EOL	6/15/23	21:30		2062		037°18.21880914'N	020°18.31764482'E	438434,058897	4128783,968553	
Line Name		Date	Time	Duration	SP	SP TOT	Lon	Lat	X	Y	Distance
POSEIDON_23_14	SOL	6/15/23	21:40	1h 50m 1s 795ms	101	385	037°18.32185669'N	020°17.26196315'E	436876,203534	4128986,109271	14379,17
	EOL	6/15/23	23:30		485		037°23.76072632'N	020°10.33490723'E	426732,962645	4139126,185342	
Line Name		Date	Time	Duration	SP	SP TOT	Lon	Lat	X	Y	Distance
POSEIDON_23_15	SOL	6/15/23	23:44	10:20	101	2190	037°24.67870080'N	020°10.47972610'E	426961,459608	4140821,707551	81951,33
	EOL	6/16/23	10:04		2290		038°00.71765957'N	020°42.86328207'E	474928,080615	4207180,601526	
Line Name		Date	Time	Duration	SP	SP TOT	Lon	Lat	X	Y	Distance
POSEIDON_23_16	SOL	6/16/23	10:13	3h 3m 5s 626ms	101	653	038°00.93283320'N	020°43.72994144'E	476197,21098	4207574,708867	24439,77
	EOL	6/16/23	13:16		753		037°58.57312301'N	021°00.13474766'E	500197,238402	4203176,444895	
Line Name		Date	Time	Duration	SP	SP TOT	Lon	Lat	X	Y	Distance
POSEIDON_23_17	SOL	6/16/23	13:29	8h 4m 2s 384ms	101	1718	037°59.23225428'N	021°01.00320572'E	501468,234735	4204395,436964	
	EOL	6/16/23	21:33		1818		038°31.27698100'N	020°43.83315149'E	476511,648891	4263689,425476	64363,12
Line Name		Date	Time	Duration	SP	SP TOT	Lon	Lat	X	Y	Distance
POSEIDON_23_24	SOL	6/18/23	15:36:46	24m 38s 48ms	101	87	038°35.78816732'N	020°30.13211176'E	456650,895866	4272115,393612	3224,89
	EOL	6/18/23	16:01:24		187		038°35.45762227'N	020°32.29926106'E	459793,156095	4271487,653238	

Line Name		Date	Time	Duration	SP	SP TOT	Lon	Lat	X	Y	Distance
POSEIDON_23_23	SOL	6/18/23	16:14:35	2h 6m 47s 678ms	94	450	038°36.26997318'N	020°32.53204778'E	460138,529956	4272988,326675	16824,70
	EOL	6/18/23	18:21:23		543		038°43.83190428'N	020°26.54600378'E	451536,56729	4287021,630345	
Line Name		Date	Time	Duration	SP	SP TOT	Lon	Lat	X	Y	Distance
POSEIDON_23_22	SOL	6/18/23	18:48:37	1h 26m 43s 545ms	101	301	038°45.20048495'N	020°27.36774752'E	452742,038163	4289545,598458	11245,58
	EOL	6/18/23	20:15:21		401		038°45.75469833'N	020°34.98414401'E	463776,806631	4290512,696654	
Line Name		Date	Time	Duration	SP	SP TOT	Lon	Lat	X	Y	Distance
POSEIDON_23_21	SOL	6/18/23	20:16:43	1h 33m 42s 251ms	101	333	038°45.85026941'N	020°35.03697107'E	463854,104619	4290689,102765	12441,71
	EOL	6/18/23	21:50:26		433		038°51.48553787'N	020°30.70154278'E	457632,145441	4301142,397154	
Line Name		Date	Time	Duration	SP	SP TOT	Lon	Lat	X	Y	Distance
POSEIDON_23_20	SOL	6/18/23	21:51:51	2:03	101	430	038°51.57844230'N	020°30.72491919'E	457666,86779	4301314,042057	16079,76
	EOL	6/18/23	23:54:51		530		038°53.91054310'N	020°41.15438605'E	472763,246247	4305561,001428	
Line Name		Date	Time	Duration	SP	SP TOT	Lon	Lat	X	Y	Distance
POSEIDON_23_19	SOL	6/18/23	23:55:54	2:03	101	434	038°53.99045092'N	020°41.17615903'E	472795,222027	4305708,682022	16232,53
	EOL	6/19/23	1:58:02		534		039°00.70207454'N	020°34.25973281'E	462857,798727	4318162,615115	
Line Name		Date	Time	Duration	SP	SP TOT	Lon	Lat	X	Y	Distance
POSEIDON_23_18	SOL	6/19/23	1:59:54	6h 26m 32s 718ms	101	1375	039°00.68550638'N	020°34.07986156'E	462598,105052	4318133,199365	51432,50
	EOL	6/19/23	8:26:27		1475		038°35.95775652'N	020°17.94925403'E	438971,389242	4272544,42073	
Line Name		Date	Time	Duration	SP	SP TOT	Lon	Lat	X	Y	Distance
POSEIDON_23_25	SOL	6/20/23	20:07:30	9:49	101	2174	037°22.01393823'N	019°56.49366195'E	406277,27507	4136100,359315	81468,36
	EOL	6/21/23	5:56:04		2274		037°58.23560491'N	020°27.36510392'E	452226,483091	4202691,824191	
Line Name		Date	Time	Duration	SP	SP TOT	Lon	Lat	X	Y	Distance
POSEIDON_23_26	SOL	6/21/23	6:02:07	3h 39m 27s 268ms	101	811	037°58.66292323'N	020°27.56989032'E	452530,854533	4203480,28142	30374,71
	EOL	6/21/23	9:41:35		911		038°03.70275476'N	020°08.35702159'E	424494,090594	4213011,855593	
						24724					925682,0348